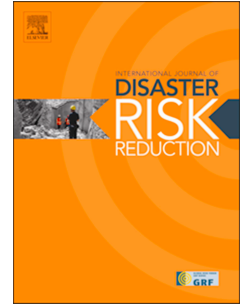


Journal Pre-proof

Evaluating Multi-Hazard Preparedness for a Major Earthquake: A Case Study of Tabriz City (NW Iran)

Mohammad Ghasemi, Saman Ghaffarian, Sadra Karimzadeh, Masashi Matsuoka, Hiroyuki Miura, Bakhtiar Feizizadeh



PII: S2212-4209(24)00848-3

DOI: <https://doi.org/10.1016/j.ijdr.2024.105086>

Reference: IJDRR 105086

To appear in: *International Journal of Disaster Risk Reduction*

Received Date: 24 May 2024

Revised Date: 9 December 2024

Accepted Date: 10 December 2024

Please cite this article as: M. Ghasemi, S. Ghaffarian, S. Karimzadeh, M. Matsuoka, H. Miura, B. Feizizadeh, Evaluating Multi-Hazard Preparedness for a Major Earthquake: A Case Study of Tabriz City (NW Iran), *International Journal of Disaster Risk Reduction*, <https://doi.org/10.1016/j.ijdr.2024.105086>.

This is a PDF file of an article that has undergone enhancements after acceptance, such as the addition of a cover page and metadata, and formatting for readability, but it is not yet the definitive version of record. This version will undergo additional copyediting, typesetting and review before it is published in its final form, but we are providing this version to give early visibility of the article. Please note that, during the production process, errors may be discovered which could affect the content, and all legal disclaimers that apply to the journal pertain.

© 2024 Published by Elsevier Ltd.

1 Evaluating Multi-Hazard Preparedness for a Major Earthquake: A Case Study of 2 Tabriz City (NW Iran)

3 **Mohammad Ghasemi^{1,2}, Saman Ghaffarian^{3,*}, Sadra Karimzadeh^{1,2,4,*}, Masashi Matsuoka⁴, Hiroyuki
4 Miura⁵, Bakhtiar Feizizadeh^{1,2}**

5 ¹ Department of Remote Sensing and GIS, University of Tabriz, Tabriz 5166616471, Iran

6 ² Remote Sensing Laboratory, University of Tabriz, Tabriz 5166616471, Iran

7 ³ Department of Risk and Disaster Reduction, University College London, United Kingdom

8 ⁴ Department of Architecture and Building Engineering, Institute of Science Tokyo, 4259-G3-2 Nagatsuta,
9 Midori-ku, Yokohama 226-8502, Japan

10 ⁵ Department of Advanced Science and Engineering, Hiroshima University, Kagamiyama 1-4-1, Higashi-
11 Hiroshima, Hiroshima 739-8527, Japan

12 *Authors to whom correspondence should be addressed.

13 14 **Abstract**

15 Tabriz, a key economic and political hub in Iran, is highly susceptible to a range of natural hazards, particularly
16 earthquakes and landslides. This study develops a multi-hazard risk scenario – combining earthquake, triggered
17 landslides, and their cascading impacts on road transportation – to assess the potential impact of a 7.3 magnitude
18 earthquake on the city’s infrastructure and emergency response systems. Using a GIS-based hazard model
19 integrated with demographic and structural data, we analysed the impacts of earthquakes and landslides on road
20 accessibility, mortality rates, and the effectiveness of disaster relief efforts. The findings reveal that Tabriz’s
21 emergency response capabilities and main roads, particularly in the northern districts, would be critically impacted
22 by both the earthquake and subsequent landslides, resulting in significant delays in rescue operations and a high
23 loss of life. Up to 30% of the city’s buildings are at risk of collapse, with the most vulnerable populations —
24 including children, women, and low-income communities—facing the greatest risk. The projected death toll could
25 reach 17%, with casualties rising further if emergency response is delayed. Moreover, areas previously considered
26 relatively safe from seismic risks may still suffer substantial damage due to landslides. This study underscores the
27 urgent need for enhanced disaster planning and response taken into account the cascading effects of earthquake.
28 It also highlights the importance of reinforcing urban planning, upgrading emergency infrastructure, and raising
29 public awareness to mitigate future risks.

30

31 **Keywords:** GIS; KHM; multi-criteria analysis; geospatial techniques; sustainable development; vulnerability

32

33 1. Introduction

34 Earthquakes are among the deadliest natural hazards, frequently impacting major cities, causing substantial
35 damage to buildings, and resulting in significant loss of life [1-2]. Reports from the United Nations highlight a
36 rising frequency and intensity of earthquakes, leading to increasing damage. These trends clearly demonstrate the
37 importance of assessing earthquake preparedness at the building level to minimise losses and fatalities. A
38 comprehensive approach to earthquake preparedness must address all aspects of seismic hazards [3]. This includes
39 evaluating the quality of construction, designing and implementing earthquake-resistant structures, and
40 developing effective emergency response plans. Furthermore, it is essential to address the social, economic, and
41 environmental impacts of earthquakes in line with Sustainable Development Goal 11 (SDG 11), which aims to
42 create inclusive, safe, resilient, and sustainable cities and communities. The United Nations' SDGs, particularly
43 SDG 11, focus on reducing the impact of natural hazards such as earthquakes on society and the environment.
44 Urban areas are vital to global development, and their growth must be managed to ensure long-term sustainability
45 for both current and future generations. SDG 11 encompasses ten key targets [4-5], including:

- 46 • SDG 11.1: Ensuring safe and affordable housing, including upgrading slums.
- 47 • SDG 11.5: Reducing disaster-related deaths and impacts, with a focus on protecting vulnerable groups.
- 48 • SDG 11.9: Implementing policies that promote inclusion, resource efficiency, and disaster risk reduction.

49 This study contributes to progress on SDG 11.1, 11.5, and 11.9 by addressing earthquake preparedness and urban
50 resilience.

51 Assessing earthquake preparedness at the building level necessitates consideration of multiple factors, including
52 the building's age, construction materials, design, and location [6]. This is particularly critical for older buildings,
53 which are more susceptible to significant damage due to outdated construction practices. Moreover, earthquake
54 preparedness should involve the development of emergency response plans at both the building and city levels to
55 mitigate risks and minimise loss of life during disasters.

56 In urban emergency planning, adopting a comprehensive approach that incorporates multi-hazard analysis,
57 including the consideration of cascading effects, is essential. The concept of multi-hazard analysis recognises that
58 hazardous events can occur simultaneously, potentially leading to interconnected and cascading effects and
59 compounded challenges [7-8]. By integrating preparedness measures for various hazards, cities can strengthen
60 their resilience and response capabilities. Establishing clear and well-marked evacuation routes based on
61 accessibility measures is vital, as these pathways guide residents and visitors to safety during emergencies.
62 Providing safe and accessible shelters is equally important, as these facilities offer temporary accommodation for

63 individuals displaced during disasters. Key considerations for shelters include their proximity to hazard-prone
64 areas, capacity, and availability of basic necessities. Effective communication and transportation are the backbone
65 of emergency response. Cities must develop robust networks that connect emergency services, first responders,
66 and relevant agencies, ensuring rapid and coordinated action. Multi-hazard scenarios pose significant risks to
67 urban areas, with impacts extending far beyond physical damage to buildings and infrastructure [9-11]. Such
68 hazards can lead to fatalities, particularly in case of building collapses or when individuals are caught in hazardous
69 situations. Survivors may sustain injuries caused by falling debris, structural failures, or panic during the event.
70 Access to medical care and emergency services becomes critical in these circumstances. Furthermore, roads,
71 bridges, utilities, and communication networks can suffer extensive damage, severely disrupting emergency
72 response efforts. The repair and restoration of infrastructure are essential components of recovery. In summary,
73 effective emergency planning must account for multi-hazard scenarios, prioritise robust communication systems,
74 accessibility and strategies aimed at minimising social and economic consequences. By emphasising
75 preparedness, cities can better protect their residents and enhance overall resilience [12-14].

76 A key element of effective emergency planning involves ensuring that communities are equipped with the
77 necessary resources and information to respond promptly and cohesively to disasters. In this regard, building
78 evacuation plans are one of the vital components of any comprehensive emergency response strategy. These plans
79 provide critical guidance on safe evacuation routes, available shelter options, and communication channels for
80 emergency responders. When well-structured and effectively implemented, evacuation plans can significantly
81 reduce the risk of injuries and fatalities during disasters [15-16]. Streets and roads play an indispensable role
82 during and after earthquakes by enabling search and rescue operations, access to essential facilities, and safe
83 evacuation routes. However, earthquakes can result in significant blockages on streets and roads, creating severe
84 challenges for emergency response efforts and escalates the overall impact of the disaster. These blockages may
85 be caused by debris from collapsed buildings, landslides, and ground fissures [17-18]. The extent of such
86 blockages and their impact on critical infrastructure – such as hospitals, water treatment facilities, and other
87 essential services – can be substantial and long-lasting. Therefore, understanding the nature and implications of
88 street and road blockages is crucial in devising effective and efficient earthquake preparedness and response plans
89 [19-22]. The impact of earthquake on transportation networks and the resulting disruptions pose significant
90 challenges for emergency responders. Strategic planning, resilient infrastructure development, and heightened
91 community awareness are vital considerations for mitigating these effects and enhancing disaster response
92 capabilities.

93 Natural hazards are inherently complex and cannot be effectively addressed through a one-dimensional approach.
94 While specific hazard assessments may yield highly accurate results, they often fall short in providing
95 comprehensive guidance for planners due to the unique conditions and triggering mechanisms of each region.
96 Developing multi-hazard maps is a highly effective strategy for assessing vulnerabilities and mitigating the risks
97 associated with natural hazards. In mountainous regions, earthquakes can trigger landslides, resulting in road
98 blockages and extensive damage that complicate rescue operations. Landslides, as mass movement events, pose
99 significant threats to human safety, the environment, and the economy [23-26]. Over recent decades, Geographic
100 Information Systems (GIS) have been extensively utilised for studying natural hazards. Skilodimou et al. [27]
101 used the hierarchical method within a GIS framework to produce a multi-hazard map, classifying areas according
102 to vulnerability and identifying the most suitable locations for urban development. Similarly, Rehman et al. [28]
103 employed the hierarchical method of frequency ratio within GIS to create a multi-hazard map for Muzaffarabad
104 region, demonstrating its suitability for sustainable development and economic activities. Hashemi et al. [26]
105 developed a GIS-based model to estimate earthquake-induced losses in a Tehran neighbourhood, focusing on
106 building damage assessments, with a particular emphasis on ground effects. This research underscored the
107 importance of GIS in understanding earthquake hazards and vulnerabilities within specific geographic contexts
108 [6]. Additionally, Karimzadeh et al. [1] combined radar and optical imagery with deep learning methods to identify
109 road damage caused by the Kumamoto earthquake. However, they did not thoroughly assess the preparedness
110 levels of urban areas, particularly with regards to the impacts on accessibility for rescue operations and other
111 related emergency responses.

112 Most studies have not adequately addressed the importance of multi-hazard assessments, often focusing on
113 hazards in isolation. This approach overlooks the complex interplay of multiple factors, as many studies
114 concentrates solely on the effects of earthquakes on mortality and structures, as well as impacts of floods and
115 landslides in isolation [29-32]. However, in mountainous regions, a comprehensive assessment must consider
116 multi-hazard scenarios, Currently, no studies provides an in-depth analysis of the combined impact of landslides
117 and earthquakes, and their cascading effects on roads. This research aims to address this gap by investigating the
118 combined and cascading effects of earthquakes and landslides on both buildings and roads. The main contributions
119 of this study are threefold; (i) it integrates the Karmania Hazard Model (KHM) with the Analytical Hierarchy
120 Process (AHP) to enhance risk assessment methodologies by analysing the interdependencies between
121 earthquakes and landslides and their integration with other comprehensive data sets for city preparedness analysis;
122 (ii) it provides comprehensive high resolution data on road blockages and proximity analyses of emergency routes,

123 directly informing evacuation planning and identifying critical access points for effective emergency response;
124 (iii) the research offers context-specific recommendations for disaster preparedness in Tabriz, advocating for
125 policies that align with Sustainable Development Goal 11 (SDG 11) to improve urban resilience through inclusive
126 and sustainable planning practices.

127 We conducted the scenario-based data generation in three main stages: data preparation, application of the
128 Karmania Hazard Model (KHM) for a 7.3 Richter earthquake scenario, and the use of the AHP method to develop
129 a landslide risk map. The AHP method has been already used for several risk mapping exercised in the literature
130 including earthquake and landslide risk mapping [33-37]. We assessed structural damage, mortality rates, road
131 blockages following the earthquake, and their intersections with landslide-prone areas. The goal was to address
132 the lack of facilities and information in developing countries, particularly those prone to natural hazards. Iran,
133 with its insufficient and incomplete environmental data, has experienced significant management challenges
134 during disasters. This study provides a detailed examination of one of Iran's cities, highlighting its exposure and
135 vulnerability to natural hazards. By simulating a 7.3 magnitude earthquake accompanied by landslides in the
136 Tabriz mountains, the study underscores the critical need for comprehensive multi-hazard assessments, despite
137 the limitations in data availabilities and scope. This study primarily focuses on road blockages caused by debris
138 and landslides, employing a coordinated approach through GIS to tackle challenges related to street and road
139 accessibility. By doing so, it aims to save lives, identify critical damage points, minimise overall harm, and
140 streamline post-earthquake recovery efforts. Additionally, it evaluates the city's alignment with sustainable
141 development goals, revealing significant gaps in achieving urban resilience and fostering sustainable development
142 growth. Moreover, it calculates the distances of blocked routes for each structure and determines their proximity
143 to the nearest accessible road. This aspect is particularly critical for countries with limited resources to conduct
144 comprehensive regional assessments. By forecasting the extent of road blockages and availability of facilities, the
145 study facilitates improved planning and preparedness. Overall, this study is particularly relevant for
146 underdeveloped and mountainous cities, providing actionable insights for more effective planning and response
147 to multi-hazard crises through scenario-based approaches.

148

149 2. Methodology

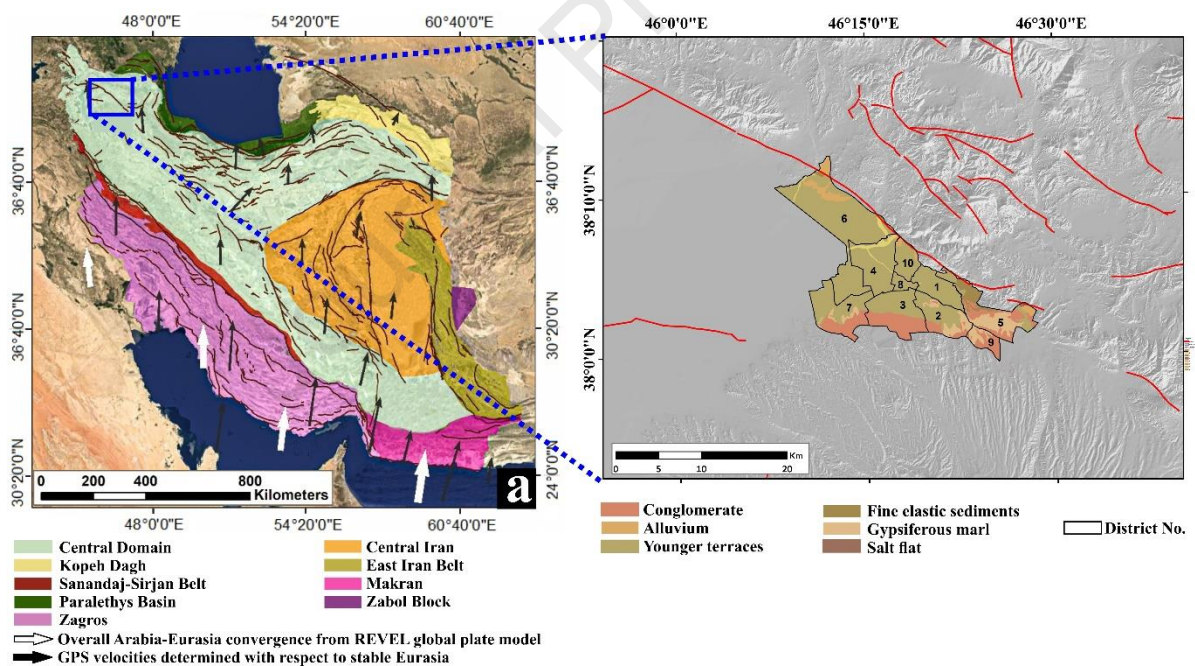
150 The methodology of this study provides a comprehensive framework for assessing earthquake-triggered multi-
151 hazard preparedness analysis for Tabriz city through an integrated geographic information system (GIS)
152 approach. It begins with a detailed analysis of the study area in Section 2.1, including geological conditions and

153 population vulnerabilities, and is followed by the development of a geodatabase in Section 2.2 that incorporates
 154 essential data from various sources. The earthquake microzonation process, described in Section 2.3, employs
 155 the Analytical Hierarchy Process (AHP) to evaluate influential parameters and generate a site amplification
 156 map. This framework is further enhanced by considering the vulnerabilities of buildings in Section 2.4, landslide
 157 risks in Section 2.5, road accessibility in Section 2.6, and population dynamics in response to potential seismic
 158 events in Section 2.7. The methods employed not only aim to improve existing hazard models but also to
 159 simulate a realistic earthquake scenario, thereby offering valuable insights into the complex and multifaceted
 160 nature of earthquake risk in Tabriz.

161

162 2.1. Study area

163 The study focuses on Tabriz city, shown in Figure 1, a major city in Iran with a population of over 1.8 million.
 164 This area is particularly vulnerable due to its proximity to the Tabriz fault in the northern region, where a highly
 165 at-risk population resides and is exposure to multiple natural hazards.



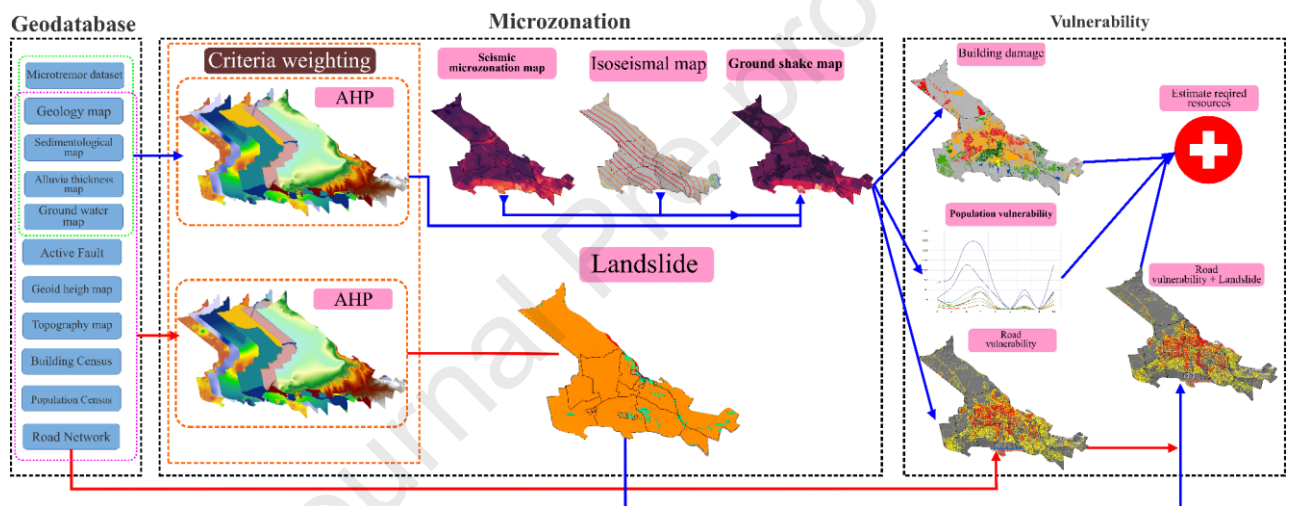
166

167 Figure 1. (a) The sedimentary and structural seismic conditions in Iran based on Aghanabati's classification (2004) [38]. (b)
 168 Spatial location of the major fault within the study area and the geological conditions of the district.

169 In this study, we used an integrated GIS approach based on spatial analysis methods to conduct a comprehensive
 170 and multidimensional analysis of the 7.3 Richter earthquake scenario [39]. Our research highlights the absence of
 171 a unified model for earthquake risk. Several methods were designed, including the Karmania Hazard Model
 172 (KHM) for Iran, designed to assess building and human damages [40]. The aim of this study is to enhance this
 173 model to improve its accuracy and realism. To achieve this, we incorporated the influence of landslide risk in

174 blocking roads, which increases the fatality rate. We prioritised the KHM as an interactive environment,
 175 combining spatial layers of building vulnerability coefficients and population data, making it suitable for
 176 earthquake scenario modelling. This model is flexible, allowing modification of spatial layers based on district-
 177 specific vulnerability coefficients, enabling the integration of road vulnerability and landslide hazards. The model
 178 has been tested and evaluated against the Bam earthquake, Sarpol-e Zahab earthquake, and the results are
 179 applicable to various environments, including both mountainous and desert regions. The general principles of our
 180 work are shown in Figure 2, which outlines three main steps, as detailed below.

181 As shown in Figure 2, this study consists of three main processes: the preparation and aggregation of information
 182 from various sources, the assessment of environmental conditions using decision-making method to evaluate
 183 earthquake risks, and the damage assessment process, all of which are described further below.



184
 185 Figure 2. The general technical process of investigating multiple risks for the city of Tabriz consists of three keys stages:
 186 obtaining information from various organizations, conducting microzonation, and assessing the vulnerability of buildings,
 187 streets/roads, and the population.

188

189 2.2. Geodatabase

190 The required data are listed in Table 1, along with the necessary information for conducting the optimised model.
 191 Field evaluations were carried out to develop and assess the Tabriz earthquake scenario, which occurred
 192 historically in 1721 with a magnitude of 7.3 on the Richter scale [41]. The GIS data layer of streets, buildings and
 193 temporary settlements were obtained, verified and corrected through ground-based surveys and official reviews.
 194 Additional information was sourced from relevant organisations, including the Crisis Management Organisation,
 195 Municipality, Surveying and Mapping Organisation, and the Planning and Budget Organisation. All layers were
 196 converted to shapefiles and integrated into a geodatabase. It should be considered that Tabriz is a large

197 metropolitan area with high-pressure electricity, gas, water and sewerage networks running beneath many of its
 198 buildings. Due to the unavailability of this data, these networks were excluded from the analysis, and it is assumed
 199 that, in case of natural hazards, they would be temporarily cut off.

200

201 Table 1. KHM Model Database for 7.3 Richter Earthquake.

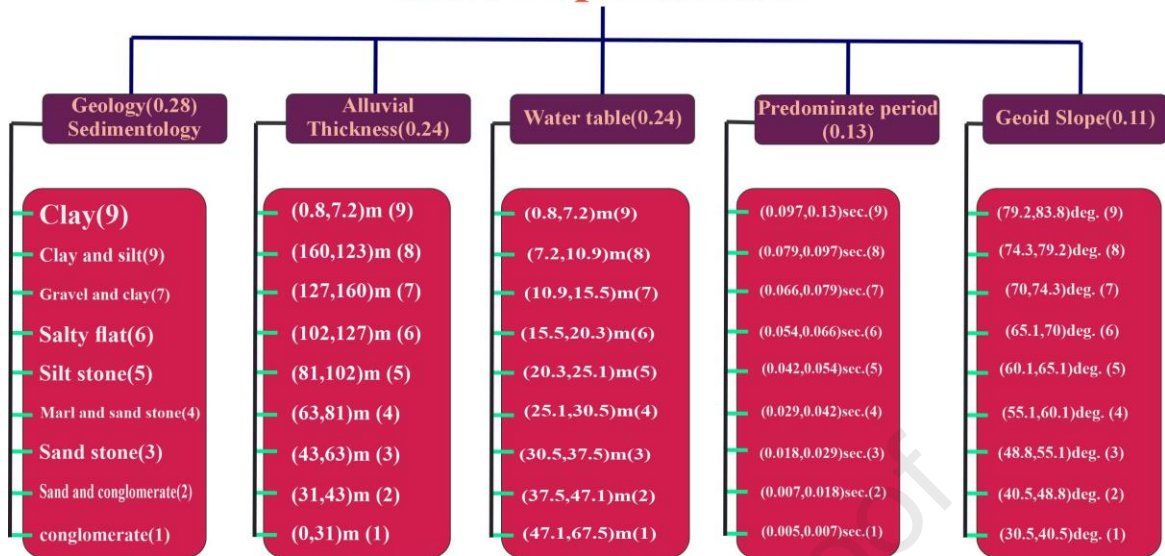
Database	Type	Source
Earthquake catalogue	vector	www.iiees.ac.ir
Active fault	vector	www.ncc.gov.ir
Ground water	raster	www.ncc.gov.ir
Geology map	raster	www.ncc.gov.ir
Sedimentological map	raster	Karimzadeh et al., 2014 (36)
Alluvia thickness map	raster	Karimzadeh et al., 2014 (36)
Microtremor dataset	raster	Karimzadeh et al., 2014 (36)
Building census	vector	www.tabriz.ir
Slope	raster	www.ncc.gov.ir
Landuse	vector	www.tabriz.ir
Topographic map	raster	www.ncc.gov.ir
Road dataset	vector	www.traffic.tabriz.ir
Landslide	vector	www.ncc.gov.ir
Population census	vector	www.tabriz.ir

202

203 2.3. Earthquake Microzonation

204 The earthquake microzonation in this study was conducted using influential data and the Analytical Hierarchy
 205 Process (AHP) decision-making model [40] (Figure 3).

Site Amplification



206

207 Figure 3. represents the weighting of parameters influencing earthquakes based on the Analytical Hierarchy Process (AHP)

208 decision-making method.

209

210 The first step involved preparing the influential parameters for seismic microzonation of the Tabriz metropolitan

211 area in the form of a comprehensive and reliable database. In this part of the study, a thorough review of various

212 research in this field, especially considering the specific conditions of the region, led to the selection of relevant

213 parameter by experts. Some parameters were omitted due to limited access to or absence of reference data. Only

214 accessible and validated parameters were used in the analysis. The selected parameters are presented in Table 1.

215 The identification of site effects on earthquakes is one of the most important factors in this model, determined

216 using various criteria [17,26,28,41,42]. The most significant factors in microzonation include geotechnical

217 characteristics [17], such as geological layers, sediment thickness, microtremors, slope, and groundwater levels.

218 These factors were utilised, and the seismic microzonation map of Tabriz was obtained through the AHP

219 weighting method. AHP is highly suitable for multi-criteria decision-making and environmental data evaluations.

220 To generate the site amplification map, the weights obtained from the hierarchical weighting method were applied

221 to the relevant layers, which were then summed together and normalised to produce the final map [41]. According

222 to expert opinion, geology was considered more important than other factors. The final site amplification

223 microzonation map was obtained using the following equation:

$$224 AI = \sum(G_i \times M_i \times T_i \times W_i \times S_i) \quad (\text{Eq.1})$$

225

226 In Equation 1, AI represents the site amplification map in a specific district, which is the sum of geological and
 227 lithological layers (G_i), seismic period of the site (M_i), sediment thickness (T_i), groundwater conditions (W_i),
 228 and topographic slope (S_i).

229 Determining seismic sources is one of the most important steps in earthquake scenario development. The fault
 230 map is prepared based on satellite images and geological maps, with active faults and seismic sources identified
 231 using aerial photos and field studies. For defining earthquake scenarios, the length, azimuth angle, and
 232 magnitude of each earthquake are measured based on fault parameters. The worst-case scenario for the most
 233 unstable fault segment is identified using Equations 2 [43] and 3 [44].

$$234 \quad M_s = \log L + 5.4 \quad (\text{Eq. 2})$$

$$235 \quad M_s = ((\log L + 0.126) / 0.675) \quad (\text{Eq. 3})$$

236 M_s represents the surface wave magnitude, and L is the fault length, typically considering 50% of the fault
 237 length.

238 Earthquake hazard at a site is typically defined based on the ground motions generated by earthquakes at that
 239 location. Its characteristics are usually determined by one or more ground motion parameters derived from
 240 empirical and theoretical relationships.

241

242 Table 2. Fault Parameters of the Earthquake Source.

NW(NTF)	Descriptions
Starting point in UTM coordinates (X, Y)	(624555.925,4213508.213)
Ending point in UTM coordinates (X, Y)	(584957.047, 423450.388)
Reference point in UTM coordinates (X, Y)	(606924.994, 422636.423)
Magnitude (Mw)	7.3
Length (km)	45
Strike (deg.)	270
Dip (deg.)	90

243

244 Subsequently, using the data from Table 2, we simulate the main fault of Tabriz with the characteristics
 245 matching those of the 1721 earthquake. Additionally, the distance relationship of each cell is described by a
 246 source, and this distance is used as the corresponding attenuation coefficient. The distance is measured from the
 247 fault up to 150 kilometres. In this study, we employ Modified Mercalli Intensity (MMI), which is derived using

248 region-specific formulas to determine the earthquake intensity. Intensity attenuation in relation to distance from
 249 the epicentre has been studied extensively, and specific coefficients have been applied for different areas.
 250 Research on attenuation in Iran has been conducted, with the most significant studies, used in this research,
 251 presented below. The following equations, derived from Ambraseys, Melville, and Chandra, were calculated for
 252 the study area range [45]:

253

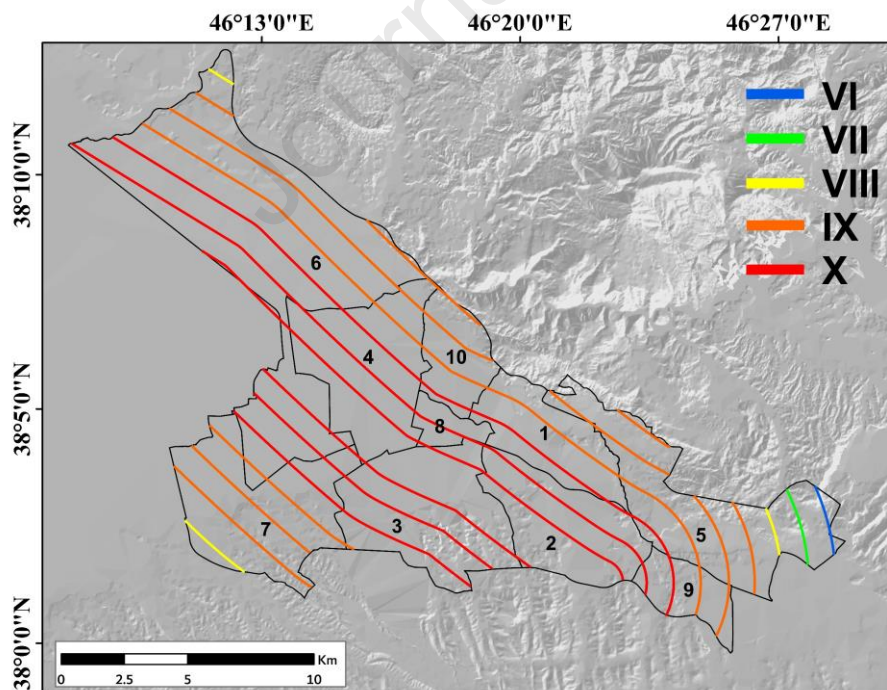
$$254 \quad I_0 = 1.3M_s + 0.09 \quad (\text{Eq. 4})$$

$$255 \quad I = I_0 + 0.453 - 0.00121R - 4.96 \log(R + 20) \quad (\text{Eq. 5})$$

256

257 In Equation 4, 5, I represent the intensity at a distance of R kilometres from the surface fault, and M_s represents
 258 the earthquake magnitude on the surface wave scale.

259 The attenuation relationships indicate the level of earthquake intensity that each point within the affected area
 260 can withstand. Since these relationships are based on PGA (Peak Ground Acceleration) and PGV (Peak Ground
 261 Velocity), and considering that the vulnerability curve of Iran's structures was derived from Modified Mercalli
 262 Intensity (MMI), the PGA, PGV method was not used. The attenuation relationships were derived using
 263 Equation 1 to obtain MMI (Figure 4).



264

265 Figure 4. Intensity map of a 7.3 magnitude earthquake (the Roman numerals represent the Modified Mercalli Intensity).

266

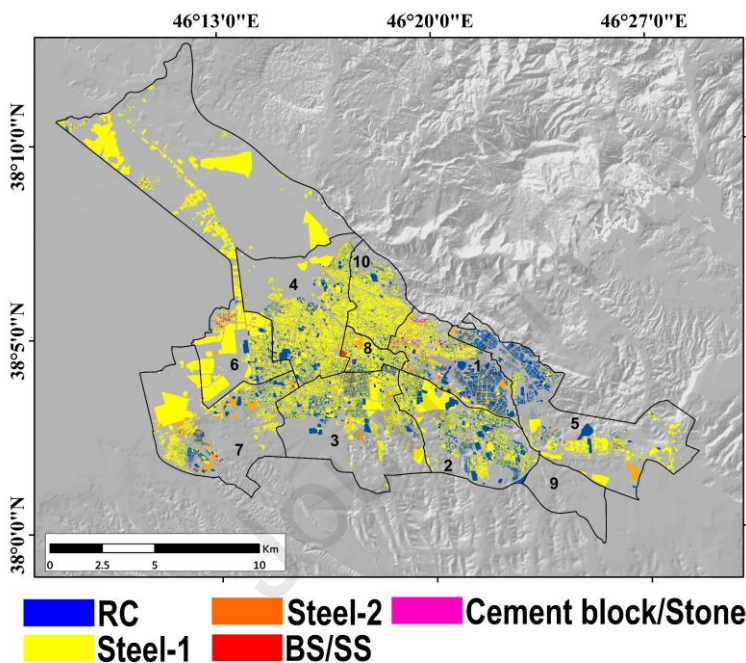
267 To generate the final ground shaking map based on the MMI scale, Equation 6 is applied, integrating the raw
 268 earthquake intensity map from Figure 1 with the detailed site classification map (Figure 4).

$$269 \text{ GSM} = \sum M_i \times I_i \text{ (Eq. 6)}$$

270

271 2.4. Buildings vulnerability assessment

272 Buildings are constructed differently across countries, resulting in varying responses to earthquakes. Numerous
 273 studies have been conducted to assess the vulnerability of buildings, taking into account their distinct construction
 274 methods. For instance, the 2008 JICA study developed vulnerability curves for Iranian buildings, drawing on data
 275 from previous earthquakes. These curves are developed based on the Modified Mercalli Intensity (MMI) scale
 276 and classify buildings according to their construction type and number of floors [46].



278 Figure 5. The distribution of buildings within the studied area in terms of their structural types, with predominant type being
 279 Steel-1, which consists of metal structures of up to three storeys.

280

281 The building map was prepared by the Housing and Urban Planning Organization. Given the slow pace of data
 282 updates in a country like Iran, the received data was thoroughly reviewed and revised to align with the latest
 283 changes. Table 3 and Figure 5 show the status of structures in Tabriz city. RC (Reinforced Concrete) buildings
 284 vary in number of storeys. The highest density is observed in districts 2 and 5, while the lowest in district 10,
 285 which accounts for only 6.4% of the total. Approximately 19.5% of the city's structures are reinforced concrete
 286 buildings. Steel-1 buildings, which are metal structures with up to three storeys, and are most common in district

287 4, where they represent 84% of the structures. Steel-1 buildings dominate Tabriz, comprising 70.8% of the total.
 288 Steel-2 buildings are metal structures with more than three storeys, with the highest proportion found in district
 289 2, making up 35% of Steel-2 buildings and 7.5% of the total in Tabriz. BS/SS refers to structures with masonry
 290 walls, typically older buildings located in suburban areas. District 1 has the highest proportion of BS/SS structures,
 291 accounting for 9.4%, mostly located in the outskirts of Tabriz. These buildings are highly vulnerable to
 292 earthquakes and pose significant risks to access routes. Cement block structures, which are constructed entirely
 293 from cement blocks, are relatively rare. Figure 5 illustrates the spatial distribution of various structural types,
 294 showing that the northern districts of Tabriz and a much of district 4 have dilapidated and vulnerable buildings.
 295 District 5, managed by Tabriz Municipality, is in a better condition, with newer buildings and a more affluent,
 296 educated population. However, district 10 and the western part of district 1 feature inadequate structures, inhabited
 297 by vulnerable populations, including migrants from surrounding villages. These areas have been marginalised,
 298 lacking basic facilities, city services, and accessibility.

299 As shown in Figure 5, the southern part of Tabriz demonstrates a highly favourable condition, exhibiting
 300 significant resistance to earthquakes. District 2 and 3 also show relatively favourable conditions., with the eastern
 301 part of district 5 being in better shape than its western counterpart. On the other hand, the central and northern
 302 parts of Tabriz, especially district 1-10, are in very unfavourable conditions and have low resistance. These areas
 303 are characterised by their proximity to the fault line, thin soil layers, loose soil, and poor geological conditions.
 304 District 9, a newly established areas designed in line with the city's engineering and developmental goals, is
 305 sparsely populated but has favourable conditions and aligns with the objectives of the Sustainable Development
 306 Goals (SDGs).

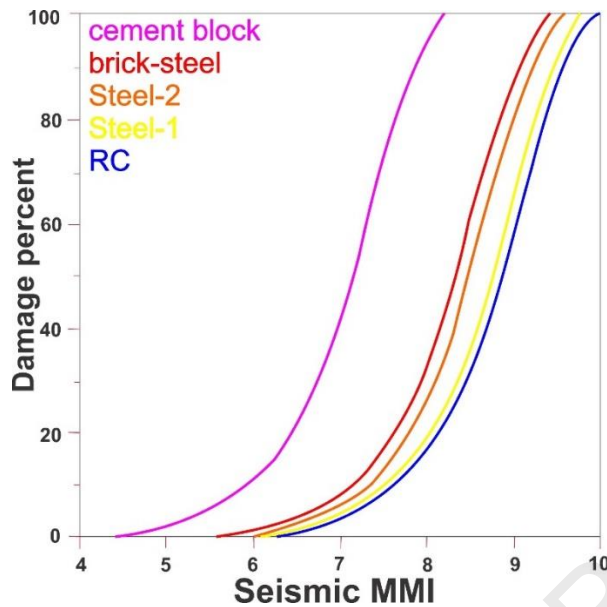
307

Table 3. Percentage distribution of types of urban structures based on each urban area

	RC%	Steel-1%	Steel-2%	BS/SS%	Cement block%
District 1	21.4	62.0	7.2	9.4	0
District 2	33.4	31.6	35.0	0	0
District 3	26.0	68.6	5.1	0.3	0
District 4	12.3	84.7	2.4	0.6	0
District 5	54.1	38.58	7.2	0.1	0.02
District 6	13.4	76.0	5.4	4.6	0.6
District 7	17.0	78.0	5.0	0	0

District 8	15.2	78.7	5.5	0.6	0
District 10	6.4	85.2	5.1	3.3	0
Total %	19.5	70.97	7.5	2	0.03

308



309

310 Figure 6. Vulnerability Curve of Buildings based on Modified Mercalli Intensity (33, 39)

311

312 Figure 6 illustrates the percentage of damage based on Modified Mercalli Intensity (MMI) for different types of
 313 structures. According to the vulnerability curve, weaker structures such as cement block and wooden buildings
 314 are highly susceptible to even mild earthquakes, resulting in significant damage. At an intensity level of 7, these
 315 types of structures typically sustain severe damage, often resulting in very high levels of destruction (D2). In
 316 contrast, the damage rate in other types of structures is less than 20%. Based on observations from documented
 317 earthquakes, the destruction levels were categorized into six classes. The highest level of destruction, D1, exceeds
 318 80%, while the lowest level, D6, is presented in Table 4.

319

320 Table 4. Classification of the level of building destruction based on Hassanzadeh et al.'s study (37,45).

Destruction level	Percent of damage	Description
No destruction (D6)	0-2	The structure is essentially intact, with no damage or only very minor damage
Light destruction (D5)	3-10	Very tiny cracks

Moderate destruction (D4)	11-30	5-20mm cracks are observed in the building
High destruction (D3)	31-60	> 20mm cracks are observed and some component of building such as wall are destroyed
Very high destruction (D2)	61-80	A part of roof and one building's wall is destroyed
Completely destroyed (D1)	81-100	Entire of roof and more than one building's wall destroyed

321

322 2.5. Landslide

323 Landslides are one of the hazards associated with earthquakes, especially in mountainous areas. Following an
324 earthquake, landslides are likely to occur in such areas. Given that Tabriz is located on a fault line and the soil in
325 northern Tabriz is loose and unstable, it is highly prone to landslides triggered by earthquakes. The occurrence of
326 an earthquake can further activate movement along the Tabriz fault [24]. The consequences of such an earthquake
327 can lead to rapid changes in the district, causing significant environmental and infrastructure damage, with the
328 destruction of the northern Tabriz highway being one of the most significant impacts. The largest landslide in
329 Tabriz is associated with the 1956 earthquake, with a magnitude of 7.2 on the Richter scale, which caused
330 substantial landslides [48].

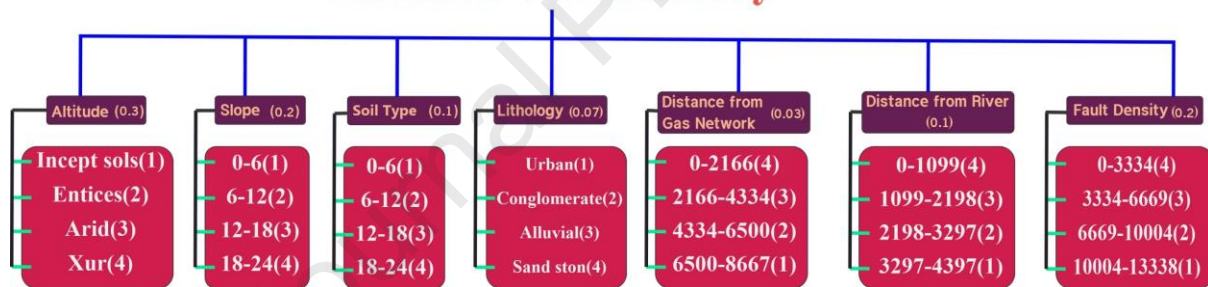
331 Since this study focuses on multi-hazards, we identified seven factors, based on expert opinions and various
332 studies, as key determinants to evaluate the city's resilience to landslides and to assess the vulnerability of the city
333 due to landslides. These factors were selected according to the study area's specific conditions and available
334 information. Landslide occurrence is determined in the GIS environment. These factors include slope degree,
335 elevation above mean sea level, distance from the fault, distance from rivers, distance from natural gas networks,
336 soil type, and lithology [27,34-36]. It is worth mentioning that the study area is considered on a local scale and
337 exhibits homogeneous conditions in terms of climatic variables. As a result, the precipitation criterion was
338 excluded (Figure 7). The AHP method was then employed to generate a landslide susceptibility map [49]. The
339 classifications of 'low,' 'moderate,' and 'high' susceptibility on the final landslide map were established using the
340 natural break (Jenks) method. This statistical approach identifies optimal breakpoints within the susceptibility
341 data, grouping similar values while maximizing the difference between classes. Consequently, areas are

342 categorised based on their relative susceptibility levels, with each class representing a distinct range of
 343 susceptibility scores derived from AHP analysis. This method allowed us to delineate susceptibility levels
 344 meaningfully and based on inherent data distributions.

345 We have adopted a classification-based approach to estimate the impact on road accessibility across varying
 346 sensitivity levels. Specifically, areas classified as high-sensitivity zones are assumed to experience complete road
 347 blockages, rendering all routes impassable. For medium-sensitivity areas, an estimated 50% of road segments are
 348 considered blocked, reflecting moderate but significant disruption. Conversely, roads within low-sensitivity zones
 349 are anticipated to remain fully accessible, as these areas are less prone to landslide impacts. This classification
 350 method provides a structured, assumption-based framework to assess road blockage severity due to landslides,
 351 leveraging sensitivity zoning to systematically estimate and convey the degree of exacerbation. These levels allow
 352 for a clear interpretation of landslide effects on road infrastructure, supporting a quantifiable measure of landslide-
 353 induced road damage that can be further validated with additional data in future studies.

354

Landslid Vulnerability



355

356 Figure 7: Weighting of parameters influencing landslide susceptibility using the Analytic Hierarchy Process (AHP) decision-
 357 making method.

358

359 2.6. Road blockage

360 Roads are considered as a key factor in emergency response and play a crucial role in traffic control and rescue
 361 operations. The presence of any structure alongside the road can cause road blockages. Open spaces and wide
 362 streets have a lower vulnerability to earthquakes, as mentioned in the structural section. North Tabriz faces a
 363 particularly challenging situation with a concentration of informal settlement and substandard shelters with
 364 minimal facilities. Due to the high building density in many areas, roads are not suitable for vehicle access, as
 365 observed during field studies. After an earthquake, roads could become blocked by building rubble and debris,
 366 which is especially critical in marginal areas where the narrowest streets are located (districts 1-10) and in district

367 4, due to its aged urban fabric that lacks proper infrastructure. Tabriz's historical district (district 8) also features
 368 narrow streets that complicate access. This study uses the following method to assess the level of road blockage:

369

370 $\text{Volume of building} = \text{Area of ground floor} \times \text{Number of stories} \times \text{Height of each floor}$ (Eq. 6)

371

372 In Tabriz, two types of construction exist: illegally constructed spaces in marginal areas with no yards, accounting
 373 for 100% of the constructed land; and structures built according to engineering standards, where 60% is built-up
 374 area and 40% is yard. This study considers the latter case. Equation 6 calculates the volume of the building, and
 375 Equation 7 calculates the volume of construction materials for each building developed by local civil engineers
 376 [26]. The demolition coefficient is then applied, and Equation 8 calculates the volume of debris.

377

378 $\text{Volume of construction materials} = \text{Volume of building} / 5$ (Eq. 7)

379

380 $\text{Volume of waste materials} = \text{Volume of construction materials} \times \text{Percent of building damage}$ (Eq. 8)

381

382 $\text{Area of waste materials} = (\text{Volume of waste materials}) / (\text{Height of waste materials})$ (Eq. 9)

383

384 To calculate the area occupied by debris, an assumed height of 1 meter is considered, and Equation 9 is applied.
 385 Finally, the area of streets occupied by debris from each adjacent building is calculated using Equation 10. It is
 386 also important to consider the distance between the building and the street [50]. The direction of collapse is taken
 387 into account as well. For example, if a building is blocked on three sides but open at the front, the debris will fall
 388 towards the front only. However, if the building is open on three sides, the debris will be distributed across all
 389 three sides.

390

391 $\text{Occupied area of adjacent street} = \text{Occupied area of the adjacent street} - \text{Area of ground floor}$ (Eq.

392 10)

393

394 In the secondary section, earthquake-induced landslides impact loose soils, and the results of landslide
 395 susceptibility indicate the city's vulnerability to landslides. Therefore, the potential impact of landslides on
 396 infrastructure is considered. In fully developed areas where there is no bare soil, it is assumed that landslides will

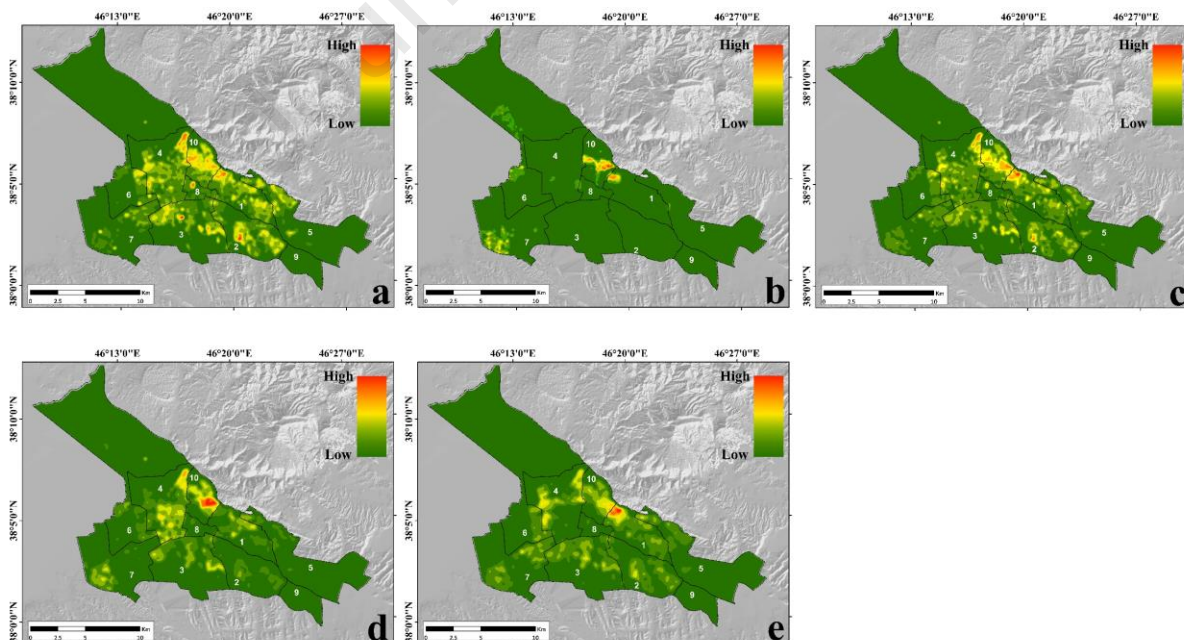
397 not significantly affect roads. In addition to these considerations, traffic movement was entirely eliminated from
 398 the analysis, with roads declared one-way due to the crisis conditions.

399

400 2.7. Population Vulnerability

401 In contemporary societies, the primary goal of emergency response is to save human lives, and in sustainable
 402 development, providing adequate shelter is considered essential. In the city of Tabriz, the population exceeds
 403 1,800,000 people. Figure 8a illustrates urban density, with 25% of the population living in marginal areas that are
 404 highly vulnerable [51]. From an economic and social perspective, housing, healthcare, urban facilities, and
 405 services are at the lowest levels of welfare, lacking access to sustainable housing, with the wealthiest class residing
 406 within a short distance of these areas. This affluent class enjoys the highest economic and social status, benefiting
 407 from better housing, healthcare, urban facilities, and services, along with ample green and recreational spaces. In
 408 terms of both structural and population density, the marginal and older areas of Tabriz, particularly district 4,
 409 exhibit high density. However, district 8 has the lowest population density but serves as Tabriz's economic hub,
 410 attracting a large influx of people from various areas during the day. The highest urban density is observed in
 411 district 10, followed by the western part of district 1 and the northern part of district 4. In terms of population,
 412 district 4 has the highest number of residents.

413



414

415 Figure 8. a) represents the population density in different areas of Tabriz municipality. b) The population density of illiterate

416 individuals in different urban areas. c) The population density of literate individuals in different urban areas. d) The

417 population density of children under ten years old in different areas of Tabriz city. e) The population density of individuals
418 above ten years old in different areas.

419

420 Population datasets are typically obtained through censuses. In this study, the statistical data from the 2020
421 yearbook of Tabriz Municipality was employed. According to Figure 8a, districts 1, 4, and 10 exhibit the highest
422 population densities among the various areas of Tabriz Municipality. Consequently, these areas also show high
423 building density, while per capita road availability is significantly lower. The average area of buildings in these
424 three districts is less than 70 square meters. Conversely, district 8, while the least populated, experiences
425 significant fluctuations in population density throughout the day, making it the busiest area with predominantly
426 commercial activity.

427 In Figure 8b, the population density of illiterate individuals is higher in districts 1 and 10. These individuals
428 typically work in lower-paying jobs and have migrated from surrounding villages to these districts. Figure 8c
429 illustrates the population density of literate individuals with education up to a high school diploma, which is
430 distributed across all urban areas, including suburban regions. The youth in these areas seek social mobility and
431 strive to improve their social status, influenced by the populations in other areas. Figure 8d depicts the population
432 density of children, with the highest concentration found in district 10. However, this area has the lowest
433 educational resources and green spaces, and is prone to high-risk urban settlements, making children the most
434 vulnerable age group in terms of earthquake impacts.

435 As shown in Figure 8e, the population over ten years old is distributed relatively evenly across all areas, with the
436 highest density observed in districts 4 and 10. The report utilises the findings of vulnerability functions presented
437 by JICA [46] and refers to the solutions proposed by Coburn et al. [52]. Based on JICA studies [48], the
438 relationship between fatalities caused by past earthquakes in Iran indicates that casualties remain low up to an
439 intensity of eight, at around 10%, but suddenly increase to 50-80% at intensities nine and ten. Another significant
440 difference in casualties is noted between night and day. Fatalities during nighttime, when residents are indoors,
441 are significantly higher compared to daytime, when people are outdoors or in more resilient structures, such as
442 workplaces.

443 As shown in Table 5, building destruction is categorised into six levels. Based on this classification, the
444 occupants of each category have coefficients that determine the loss rate, as presented in Table 5. At the D1
445 intensity level, the most destruction of buildings is observed, with 41% of occupants killed, while 22% remain
446 unharmed [52].

447

448 Table 5. Expected degree of casualties in each specific vulnerable district based on previous earthquakes (KDMC, 2008) [40].

Type of destruction	Status of people	Casualty rate	Type of destruction	Status of people	Casualty rate
No Destruction	Dead	0	High destruction	Dead	13
	Hospitalized	0		Hospitalized	17
	not hospitalized	1		not hospitalized	23
Light destruction	Not injured	99	Very high destruction	Not injured	47
	Dead	2		Dead	16
	Hospitalized	5		Hospitalized	22
Moderate destruction	not hospitalized	9	Completely destroyed	not hospitalized	28
	Not injured	84		Not injured	34
	Dead	4		Dead	41
	Hospitalized	9		Hospitalized	16
	not hospitalized	15		not hospitalized	21
	Not injured	72		Not injured	22

449

450 3. Results

451 3.1. Earthquake Microzonation

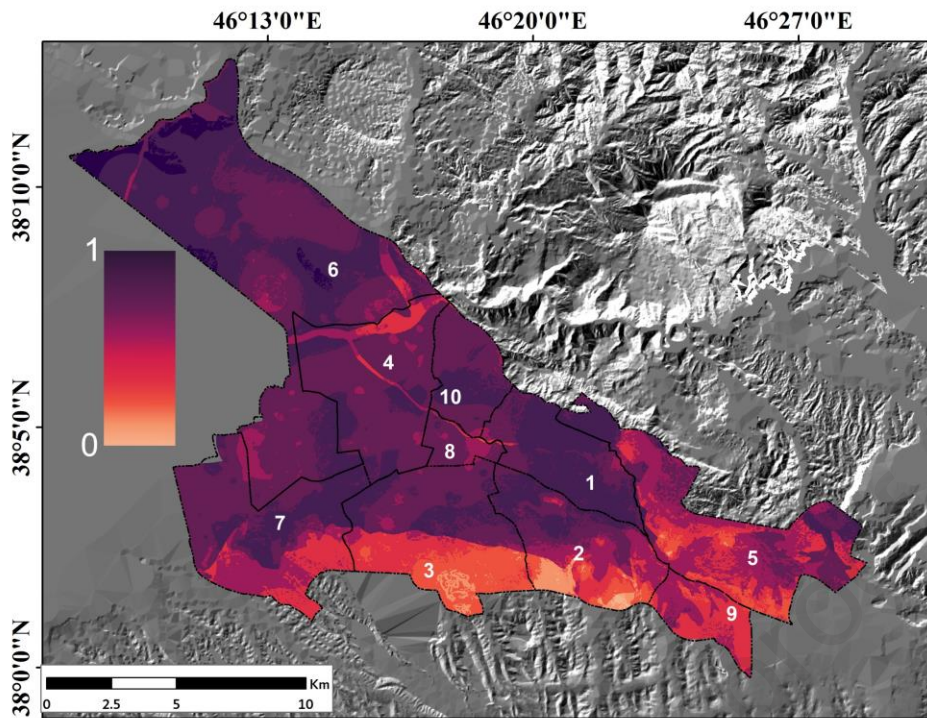
452 In this study, we updated the parameters by consulting experts, and then used the AHP weighting method to

453 prepare the site amplification. This amplification was subsequently combined with the earthquake intensity map

454 to create the ground shaking intensity map, which was used to assess the vulnerability of buildings and roads

455 (Figure 9).

456



457

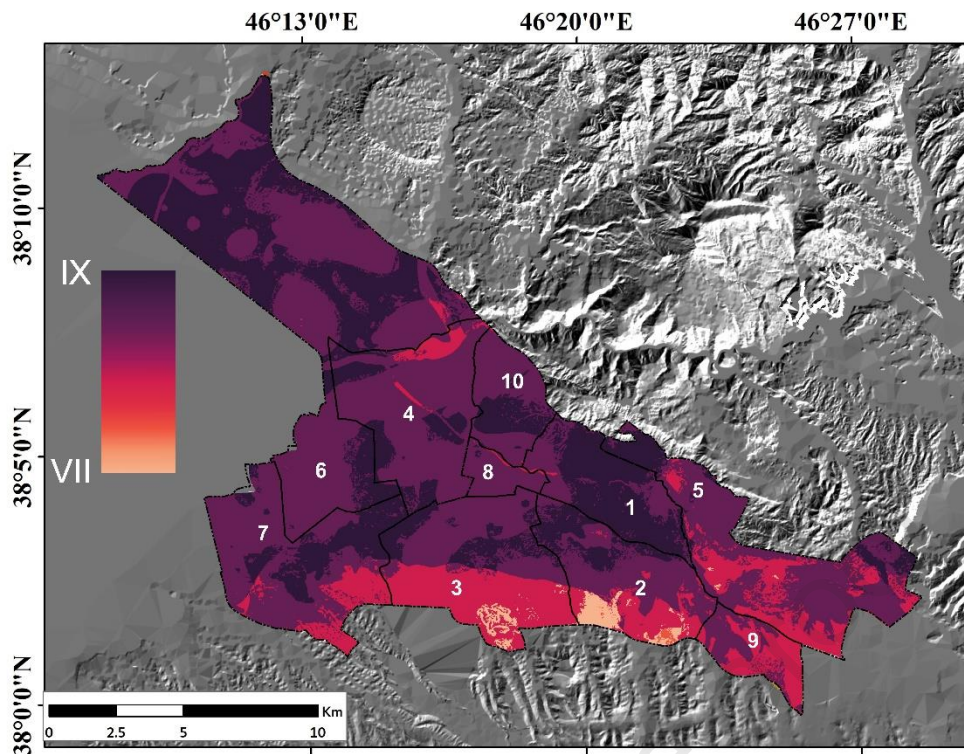
458 Figure 9. Final analytical hierarchy process adoption for the influential parameters.

459

460 Through an examination of the existing construction conditions, this study revealed that many areas within the
 461 study zone are unsuitable for development and require planning and evacuation. The expansion of Tabriz city has
 462 occurred predominantly in the northern direction, which contravenes safety principles. In contrast, the southern
 463 part of city presents a better environment for development.

464 The seismic intensity map (Figure 10) illustrates the effects of a 7.3 magnitude earthquake at its historical
 465 epicentre, aligned with the main Tabriz fault. This map highlights the impact of the raw earthquake intensity on
 466 site conditions. The marginal districts 1-10 and the western part of district 1 are projected to experience the highest
 467 level of damage, with a modified Mercalli intensity of 9. In these areas, intensity levels will peak, whereas the
 468 southern districts, as shown in Figure 10, will exhibit the lowest intensity levels, at a modified Mercalli intensity
 469 of 6. In certain areas with weak site conditions and proximity to the epicentre, damage is anticipated to be
 470 significant, with intensity levels ranging from 7 to 9. District 5 displays unique site response characteristics, while
 471 district 4, being the most densely populated urban area, will be affected by a modified Mercalli intensity of 7-9.

472



473

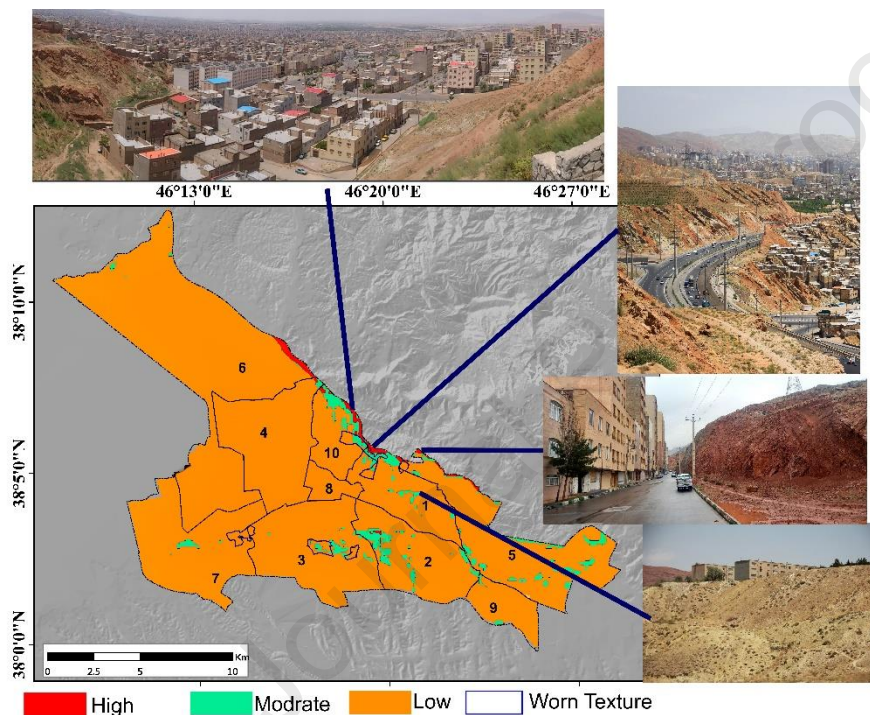
474 Figure 10. The final map of ground shaking intensity for a 7.3 Richter earthquake based on the Modified Mercalli Intensity
 475 (MMI) scale.

476 3.2. Landslide

477 Before embarking on any rescue or relief efforts, acquiring accurate environmental information is essential. In
 478 mountainous districts, landslides occur naturally but are exacerbated by human activities. While sustainable
 479 development aims to create stable environments, Tabriz city has unfortunately taken several inappropriate actions
 480 in this regard. Clearing vegetation and constructing structures on steep slopes and faults have resulted in
 481 significant damage to city's environmental resilience.

482 This study aimed to investigate multi-hazard scenarios, particularly earthquakes, landslides and their cascading
 483 effects, to assess the impacts of earthquakes on structures and various locations within the study area. The findings
 484 indicate the city's vulnerability to landslides, especially in the northern districts, including the marginal areas
 485 where unstable residential buildings have been constructed. Landslides triggered by earthquakes are among the
 486 major geological hazards in mountainous and hilly districts and represent one of the primary effects of
 487 earthquakes. Under specific conditions, post-seismic effects can be as significant as the seismic effects
 488 themselves. These conditions relate to natural slopes in active tectonic districts, where seismic shaking can weaken
 489 rock masses or soils, facilitating their descent down hillslopes and increasing erosion. Landslides involving
 490 damaged rock masses or loose soils are particularly prominent.

491 According to the results, the northern parts of districts 1 and 10 exhibit high vulnerability. District 2 also
 492 experiences high vulnerability due to the presence of steep slopes in certain areas. The central part of Tabriz city
 493 has moderate vulnerability. Figure 11 illustrates the locations of vulnerable areas, where a significant population
 494 resides near landslides and is at risk. In the event of an earthquake, these areas will face extensive damage
 495 alongside steep slopes. Additionally, developed areas in districts 1 and 5 are also exposed to landslides, as depicted
 496 in the accompanying images. As shown in Figure 11, the northern part of Tabriz has unfavourable conditions;
 497 however, the main northern highway traverses this area and has been obstructed multiple times due to landslides
 498 triggered by surrounding earthquakes. In contrast, the southern highway of Tabriz city does not pose any threats.



500 Figure 11. Vulnerability status of Tabriz city in terms of landslide susceptibility.

501

502 3.3. Building damage

503 The most significant impact of an earthquake on a city is its effect on the city's infrastructures and buildings.
 504 Regardless of the structural conditions, preserving lives and maintaining economic and social stability is
 505 paramount. Tabriz is a growing metropolis, but sustainable development in the city is progressing slowly,
 506 particularly in its northern districts. The western areas of District 1, District 5, District 2, and the northern part of
 507 District 3 are expanding, with new structures being constructed using reinforced concrete.

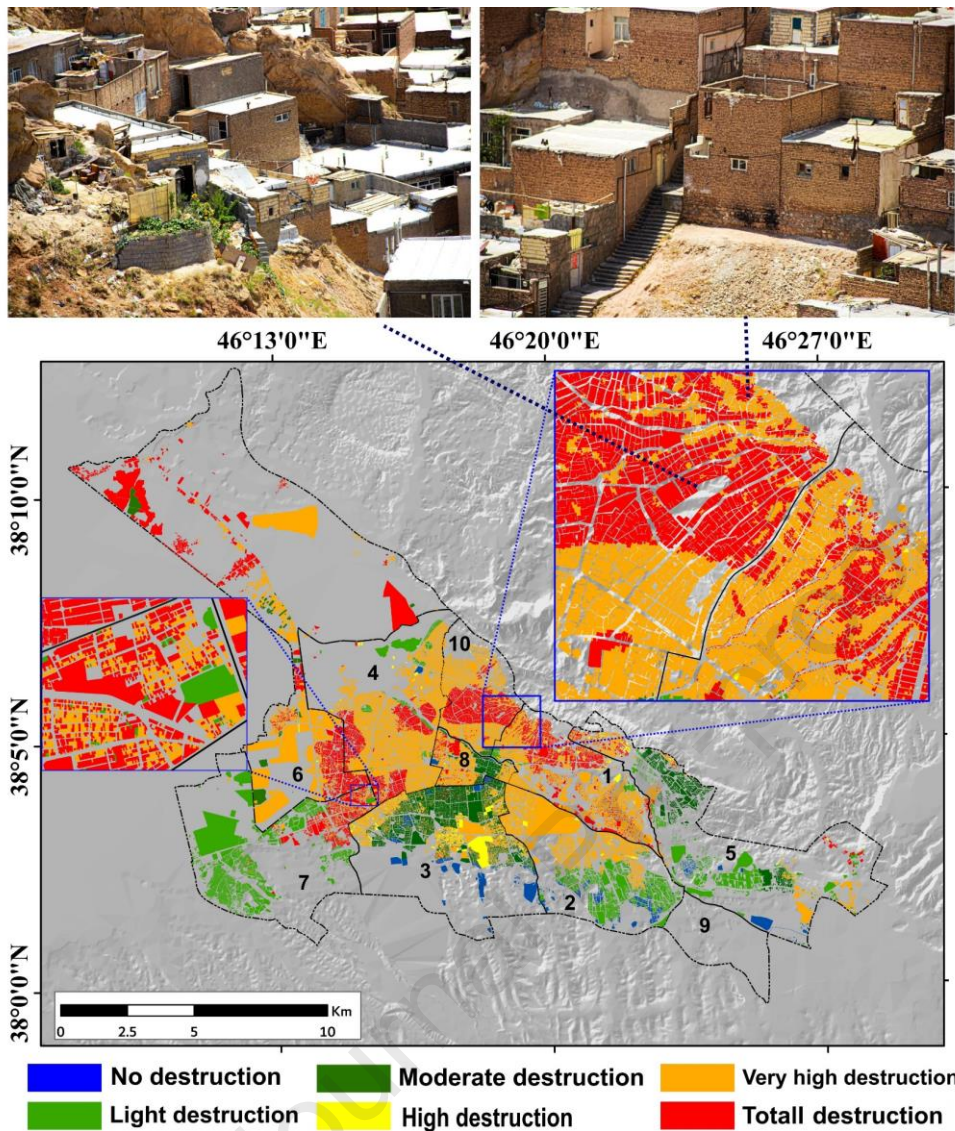
508 Structures are significantly affected by earthquakes, and the extent of damage varies depending on the Modified
 509 Mercalli Intensity (MMI) and the type of structure. In 2008, JICA developed fragility curves for Iranian structures,

510 illustrating the damage each structure may sustain based on the MMI [41, 46]. The northern part of District 3 is
511 not experienced favourable conditions regarding foundation stability and the intensity of shaking. However, with
512 building upgrades, conditions in these areas could improve.

513 Approximately 52% of the structures in Tabriz are expected to suffer destruction ranging from 60% to 100%, with
514 District 4 being the most severely affected, accounting for 75% of this damage and comprising 60,135 buildings.
515 District 1 follows with an expected 50% destruction rate. Moreover, 21% of all structures in the city will
516 experience destruction between 80% and 100%, with District 10 having the highest proportion, representing 46%
517 of the total destruction, while District 1 accounts for 43%.

518 Samples from the structural conditions in Districts 1 and 10 reveal the accessibility and structural integrity of
519 these areas (Figure 12). The lowest levels of damage are anticipated in Districts 2, 3, and 7, attributed to their
520 distance from potential earthquake epicentres, better foundation conditions, and improvements in building
521 standards. District 8, a historical and commercial hub of Tabriz, hosts a large daily population. The results indicate
522 that this district will experience significant destruction, particularly in the covered bazaar, which is characterised
523 by extensively damaged structures and the highest destruction coefficient. Providing assistance within this bazaar
524 poses considerable challenges.

525



526

527 Figure 12. Location of structural damage in the city of Tabriz during the 7.3 Richter earthquake.

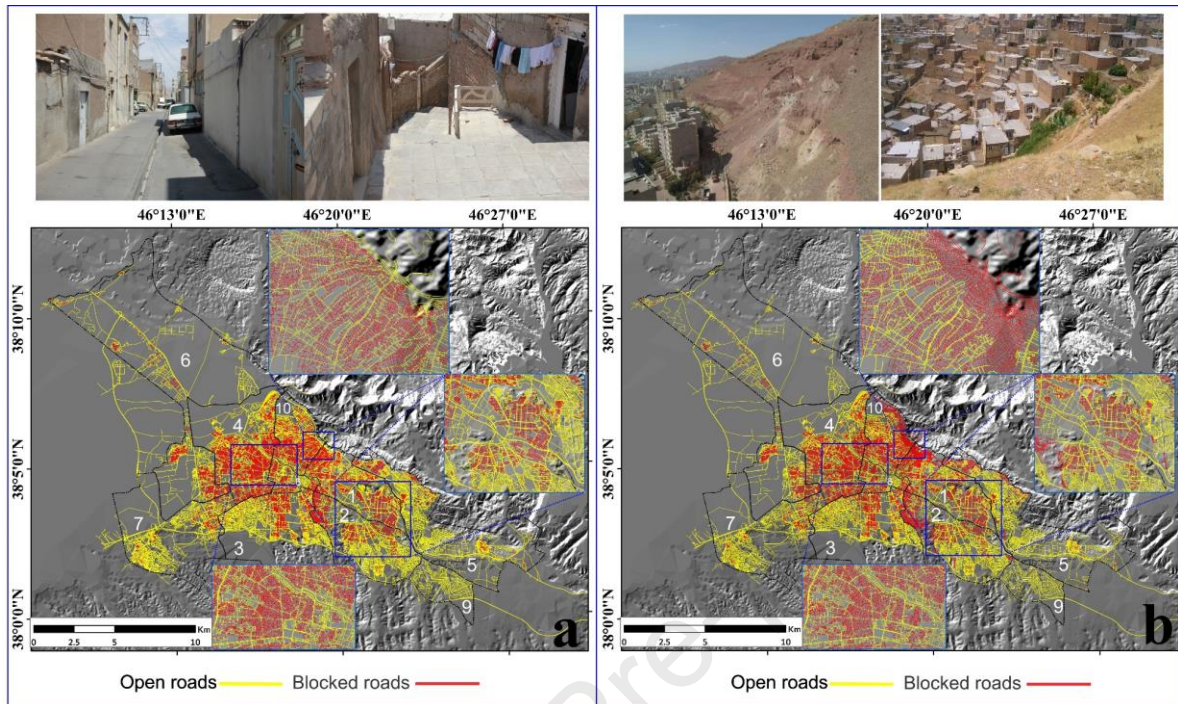
528

529 3.4. Road blockage due to building demolition and landslides.

530 Demolished buildings significantly impact road blockage and accessibility in Tabriz. There is a direct correlation
 531 between the level of destruction and the extent of road blockage throughout the city. In areas with high levels of
 532 destruction, road blockages have markedly increased. Overall, approximately 40% of the streets in Tabriz are
 533 completely obstructed, with District 4 experiencing the highest level of blockage at 60%. District 10 is similarly
 534 affected, with a blockage rate of 54%, while District 1 was also seen widespread obstructions.

535 In the eastern part of District 1, planned development and wide main streets were compromised by severe damage
 536 from buildings constructed outside of regulations. The volume of these structures has exceeded the street capacity,
 537 resulting in blockages across most thoroughfares. This district is completely surrounded by high-rise buildings,

538 and over 55% of the secondary and local roads connecting to Districts 1, 4, 8, and 10 are obstructed (see Figure
 539 13a).



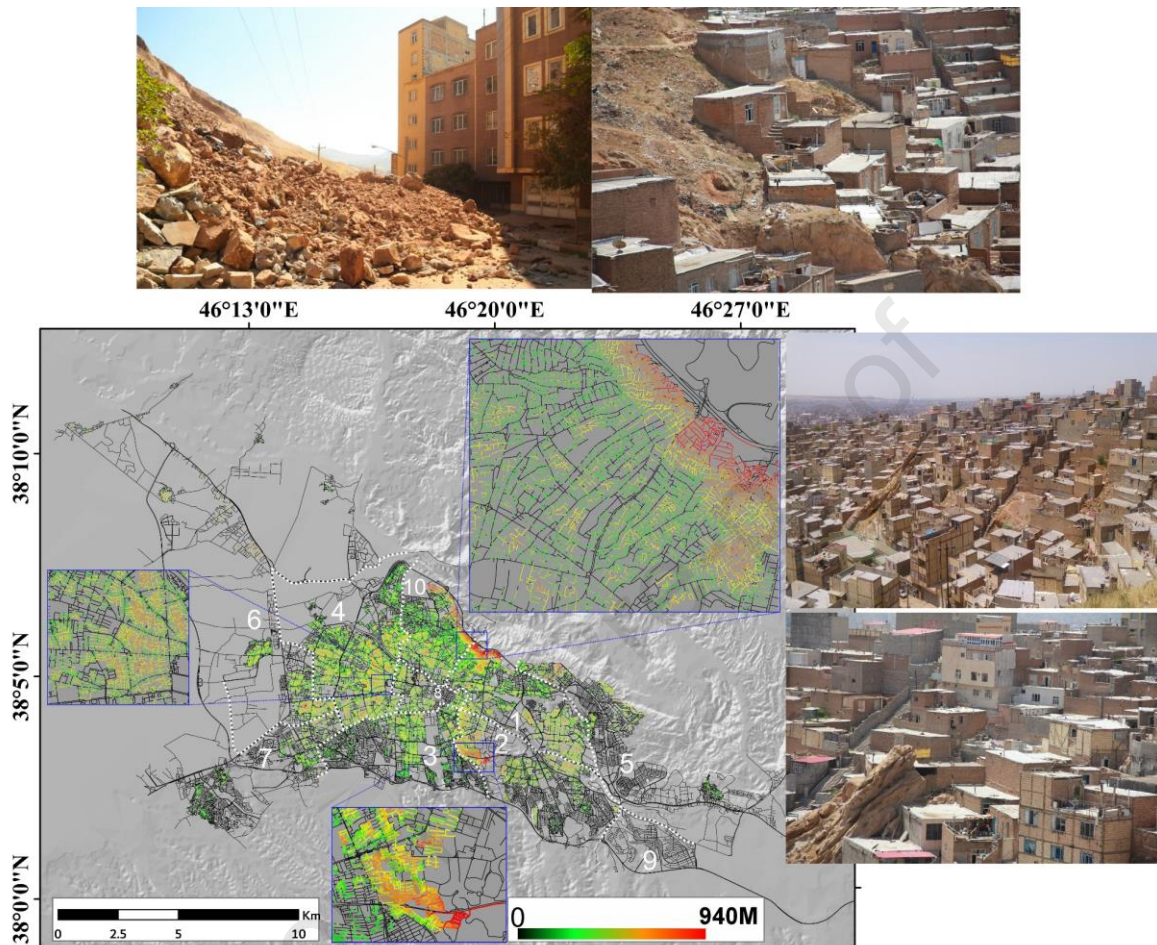
540
 541 Fig. 13. a) The status of all street blockages in Tabriz city due to an earthquake, b) The status of street blockages after a
 542 landslide scenario, indicating an increase in street blockages.

543
 544 As previously mentioned, Tabriz is a mountainous city situated near an active fault line. In the event of an
 545 earthquake, the movement of loose rocks and soil can have significant repercussions on infrastructure, particularly
 546 roads. The North Tabriz Highway, which serves as the primary access route to the northern part of the city, is
 547 particularly vulnerable to landslides. Such events can cause blockages that extend well beyond the highway itself,
 548 severely hindering access to northern areas of Tabriz, which have experienced the most damage and urgently
 549 require rescue and relief efforts.

550 The results indicating changes in street blockages due to building destruction suggest that rescue and relief
 551 operations will need to adapt significantly across many areas of Tabriz. Crisis management authorities can take
 552 proactive measures to identify sustainable solutions. Generally, following a landslide, a substantial portion of the
 553 roads may become temporarily inaccessible for rescue operations, with blockages primarily affecting main streets
 554 and complicating relief efforts.

555 District 2 of Tabriz is another area that has experienced notable changes, particularly in its western section, where
 556 steep slopes have led to blockages on multiple routes. The impact of landslides can also be observed in other

557 districts. Overall, road blockages have increased by 8%, predominantly affecting main thoroughfares (see Figure
 558 13b).
 559



560
 561 Figure 14. Distance from each blocked building to the nearest accessible road due to earthquake and landslides.

562

563 The term "vulnerability unit" refers to buildings that have sustained damage following the earthquake. The debris
 564 from these buildings obstructs roadways, while landslides further exacerbate road damage. We examined the
 565 extent of road blockages and calculated the distance from each trapped building to the nearest open road to
 566 prioritize the deployment of rescue teams and the reopening of routes for rescue operations.

567 As illustrated in Figure 14, the northern part of Tabriz has the longest distances to open roads. Given that residents
 568 in these areas are highly vulnerable and the population density is significant, evident from sample images of the
 569 marginal areas in District 1, many of these locations remain blocked even under stable conditions. Certain areas
 570 lack vehicular access altogether, with distances being steep and convoluted. The rate of building destruction
 571 exceeds 80% per day, and this figure is expected to rise, necessitating immediate rescue efforts and road clearance.

572 The total length of blocked roads requiring complete reopening is 1,560 km, with most of this distance
573 concentrated in suburban areas, where blockages exceed 500 meters in some cases and even reach more than 900
574 meters. On average, blocked buildings are located just 25 meters from open roads. The northern part of Tabriz
575 faces the most severe conditions, while the southern part is in the most favourable state. Overall, Districts 1, 4,
576 and 10 are prioritized for road reopening.

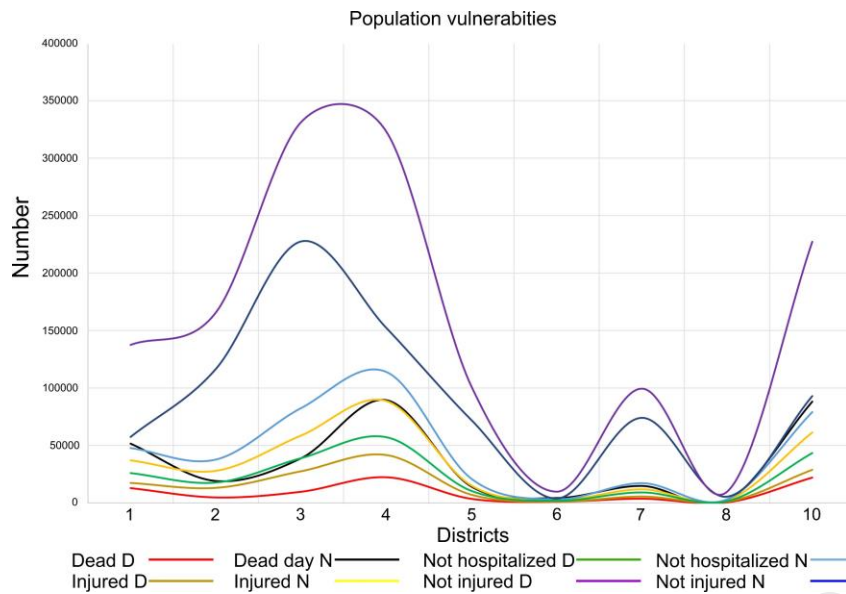
577 This level of debris presents a humanitarian crisis for a developing country. We have established a target response
578 time of 15 minutes to rescue individuals trapped under the debris each day. However, based on current conditions,
579 the prospects for effective rescue operations in Districts 1, 4, and 10 appear bleak. As time passes, victims who
580 are either trapped under the rubble or exposed to the elements will encounter increasingly dire circumstances,
581 including a lack of rescue efforts, first aid, and water, which could lead to fatalities. The longer it takes to initiate
582 rescue operations, the greater the number of victims buried beneath the debris.

583

584 3.5. Population vulnerability

585 Population vulnerability will fluctuate based on mortality rates during both day and night, as indicated by JICA
586 studies [46]. Generally, vulnerability significantly increases at night. The mortality level varies according to the
587 extent of destruction. During the night, an estimated 322,280 individuals—representing 17% of Tabriz's
588 population—are projected to perish, with this number rising in the absence of effective rescue and relief efforts.
589 Table 5 presents the mortality rates, indicating that 802,087 individuals (43% of the city's population) could be
590 rescued at night, making their assistance vital for those trapped under the rubble. This figure includes those who
591 require immediate rescue and relief, comprising 16% of the vulnerable population. These at-risk groups are
592 primarily situated in the northern and peripheral areas of Tabriz. Figure 15 illustrates the mortality rates during
593 both day and night.

594



595

596 Figure 15. Casualties resulting from a 7.2 Richter earthquake, correlated with building destruction.

597

598 According to Figure 15, if an earthquake occurs at night, approximately 90,000 people will be affected in Districts
 599 4 and 10; if it occurs during the day, this number drops to around 18,000. District 10 faces particularly challenging
 600 rescue conditions due to high levels of obstruction and the distance of each house from the nearest accessible
 601 route. In contrast, Districts 3 and 7 have the highest number of survivors, who can provide significant support
 602 during rescue operations. With open pathways, these districts are the most suitable for such efforts. District 3,
 603 with a population nearing 35,000, is poised to play a crucial role in rescue efforts.

604 In District 1, especially in the northern regions (marginal areas), the death rate is elevated due to poorly
 605 constructed buildings situated near the fault line and on steep slopes, making rescue operations difficult due to
 606 poor communication and access. The lack of open and safe spaces further exacerbates the situation. District 9 was
 607 excluded from the study due to its status as a newly established area with a very small population.

608

609 4. Discussion

610 An earthquake has destructive effects on a city, encompassing social, economic, physical, and psychological
 611 impacts. While remote sensing is highly effective in identifying post-earthquake damages, less developed
 612 countries face challenges in utilising high-resolution satellite images and advanced algorithms. In contrast, GIS
 613 have proven effective at designing prediction and scenario systems, as demonstrated in the Bam and Sarpol-e
 614 Zahab earthquakes.

615 Previous studies [24, 36, 37, 39] primarily focused on earthquake risk, building destruction impacts, and projected
616 death rates. In our study, however, we examine the effects of building destruction on route blockages, not just for
617 local roads but for all routes throughout the city. We assess the extent to which relief forces encounter roadblocks
618 from their starting points to critical areas and whether alternative routes are available. This research demonstrates
619 that relief forces positioned on the nearest routes may be unable to access affected areas due to obstructions, while
620 those stationed farther away may still be able to respond.

621 Moreover, our study highlights the impact of landslides on road accessibility, emphasising the significance of
622 determining the distance from each structure to the nearest accessible road—a calculation that can be made
623 automatically. It reveals that a significant vulnerable population is affected by earthquakes, with these areas also
624 susceptible to post-earthquake landslides. Many residents belong to vulnerable groups characterised by low
625 educational levels, low incomes, and a high number of children, making it nearly impossible for them to rebuild
626 their lives without global assistance. This support will be vital for improving their mental and psychological well-
627 being, as they lack the means to construct housing and will face conditions worse than before.

628 In Districts 1 and 10, most structures are weakly built from low-quality materials, and the narrow passageways
629 often prohibit vehicle access. These districts are situated on loose and unstable ground close to the Tabriz fault
630 line. Following the earthquake, secondary access roads in these areas have become increasingly neglected and are
631 at high risk of further earthquakes and landslides. Conversely, the eastern part of District 1 is a prosperous area
632 with a highly educated population and higher incomes, which could facilitate rebuilding efforts. However, this
633 area is not ideally located geologically, as it lies in close proximity to the main fault line and is also at risk of
634 landslides. Additionally, the altitude of the buildings exceeds allowable limits, significantly impeding effective
635 emergency response. Meanwhile, the structures in District 5 have demonstrated resilience due to their recent
636 construction; however, being located in the northern part of Tabriz—an area prone to landslides—poses a threat
637 to both main and secondary roads.

638 The density of hospitals in Tabriz is predominantly concentrated in the city centre, with districts 1, 4, 5, 8, and 10
639 identified as the most critical areas following an earthquake and subsequent landslides. Access to these districts
640 will be challenging due to prolonged blockages, which can be attributed to negligence from relevant organisations
641 and local residents. Districts 1, 5, and 10 are particularly vulnerable to landslides, leading to a significant increase
642 in blocked buildings and trapped individuals. Following the earthquake, all buildings in Tabriz were assessed for
643 their distance from the nearest accessible route. Alarmingly, these districts also have the highest population growth
644 rates and a significant number of children, who are particularly vulnerable during earthquakes.

645 The findings indicate that the most disadvantaged social class in Tabriz will face the most severe disaster, as there
646 is insufficient open space to accommodate the large population, and the nearest hospital will struggle to manage
647 the influx of casualties alone. These districts will require assistance from national and potentially international aid
648 to facilitate the relocation of their populations.

649 District 5 is a developed urban area that has been constructed contrary to sustainable development principles and
650 is situated in highly unsuitable locations, making it susceptible to significant earthquake damage and extensive
651 landslides. District 8, known for its historical significance, contains the world's largest covered market/bazaar,
652 which is likely to suffer severe damage. Rescue operations in this area will be particularly challenging, as the use
653 of heavy machinery will be limited. The destruction of this UNESCO World Heritage site would be catastrophic,
654 particularly as many of its streets are only 2 meters wide and the buildings are in a deteriorating state.

655 Conversely, District 2 benefits from better natural conditions and is less affected by earthquakes. However, areas
656 with poor building conditions are likely to face substantial destruction. Although developed regions may
657 experience less damage, they could still face access blockages following landslides. In these districts, steep slopes
658 and unstable conditions, high-rise construction instead of suitable vegetation cover, have led to become vulnerable
659 areas. The presence of an affluent population has also resulted in the development of buildings in unsuitable areas.
660 While these locations may appear suitable for temporary housing, they are heavily affected by landslides, posing
661 significant risks to human lives. The city of Tabriz does have a large stadium that could be repurposed for
662 temporary housing.

663 The results reveal that, should an earthquake occur, the city would experience serious damage and challenges for
664 relief efforts. It is recommended that fundamental revisions be made to construction methods, including
665 preventing new developments around fault lines, reinforcing structures in critical areas, preparing maps of
666 emergency evacuation routes based on existing scenarios, and increasing public awareness and preparedness. This
667 study can inform large-scale plans for critical areas, including creating walls/dams to prevent landslides from the
668 northern mountain sides. Vulnerable populations, particularly the elderly and children concentrated in high-risk
669 areas, need training to navigate crises, understand critical routes, and identify safe locations.

670 Improving the quality of life and living conditions in these areas is a national priority, and government support is
671 essential for enhancing housing and widening streets. While a limited number of schools in vulnerable areas are
672 resistant to earthquakes, most mosques in the city have been newly constructed to withstand seismic activity. Each
673 neighbourhood mosque can serve as a storage location for essential equipment that can assist trapped individuals

674 prior to the arrival of rescue forces. Training through the Red Crescent organization will be crucial, as the scale
675 of destruction will be extensive, necessitating global solutions and coordination.

676 Areas that are particularly prone to landslides should not be considered for temporary settlement. City officials
677 should prioritise locations with better accessibility and lower risk profiles for temporary housing. Our findings
678 indicate that the southern part of Tabriz is the most suitable area for establishing temporary settlements and
679 hospitals, whereas District 10 presents the worst conditions for temporary housing and should be developed near
680 District 6 of Tabriz municipality.

681 Tabriz is a historic city that has experienced devastating earthquakes. Its natural growth has often violated
682 sustainable development principles, leading to significant marginalisation and inadequate organisation.
683 Developed areas are situated in districts that will likely suffer extensive destruction. Urban green spaces have
684 been sacrificed for construction, and human activities near faults and steep slopes have exacerbated the risk of
685 landslides. The city's gas network, located beneath urban structures, further heightens these risks, contributing to
686 the potential humanitarian crisis Tabriz may face in the event of an earthquake.

687 Currently, Tabriz has 36 hospitals, each offering various specialties. However, given their limited capacity
688 compared to the expected number of casualties, establishing mobile hospitals in crisis areas prone to earthquakes
689 and landslides is essential. The northern parts of Tabriz, especially districts 1, 4, and 10, will face challenges in
690 setting up mobile hospitals due to the dense urban fabric and lack of available space. In contrast, the southern
691 areas of Tabriz boast ample open and green spaces, including football stadiums and large parks, which could
692 accommodate a significant population.

693 Districts 2 and 3 of Tabriz municipality have the highest ratios of urban green spaces, whereas districts 10 and 8
694 have the least. The results highlight that using basic or low-tech mechanical rescue tools will be extremely
695 challenging, and the high population density will result in a significant number of casualties. Rescue and relief
696 managers should consider aerial operations, modern technologies, and international assistance as primary
697 strategies. Furthermore, mosques could serve as temporary housing locations while fulfilling their religious roles
698 at the neighbourhood level.

699 The necessary facilities and equipment for providing initial aid to injured individuals were identified, though the
700 potential increase in casualties was not fully accounted for. Delays in rescue and relief efforts could reduce the
701 number of healthy individuals available to assist, necessitating additional resources. The required facilities for
702 such a scenario, as outlined in the JICA report (Table 6), were taken into consideration. In the event of a major
703 earthquake in Tabriz, with the level of destruction anticipated, immediate social support services will be essential

704 to maintain the morale of unaffected individuals. Concurrently, there is a pressing need for aerial capabilities to
 705 provide assistance to northern areas of Tabriz.

706

707 Table 6. Formulas for estimating resource requirements based on historical earthquake data [37].

Material	The formula
Total Damaged Population (TDP)	Total population-Dead people
Rescuer	$(\text{Hospitalized injuries} + \text{Injures and not hospitalized})/10$
Shovel	Rescuer + Not injured people
Emergency toilet	$\text{TDP}/20$
Emergency bath	$\text{TDP}/20$
Stick and athel	$(\text{Hospitalized injuries} + \text{Injured and not hospitalized}) \times 10$
Bandage	$(\text{Hospitalized injuries} + \text{Injured and not hospitalized}) \times 10$
Field hospital	$\text{Hospitalized injuries}/100$
Drinking water (bottle per day)	$3 \times \text{TDP}$
Canned food (per day)	$1 \times \text{TDP}$
Bread (Loaves per day)	$1 \times \text{TDP}$
Blanket	$1 \times \text{TDP}$
Tent	$1 \times \text{Family in need}$

708

709

710 Table 7. Essential facilities for a nighttime scenario of a 7.3 magnitude earthquake (derived from Table 2).

Material	Number
Total Damaged Population (TDP)	1,520,624
Rescuer	345,974
Shovel	1,513,135
Emergency toilet	7631
Emergency bath	1748875
Stick and athel	4,361,781
Bandage	4,361,781
Field hospital	3,054

Drinking water (bottle per day)	4561872
Canned food (per day)	1520624
Bread (Loaves per day)	1520624
Blanket	1520624
Tent	614301

711

712 According to Table 7, providing assistance necessitates a considerable amount of equipment, and the distribution
 713 process may be time-consuming. Therefore, it is recommended that responsible individuals prepare appropriate
 714 warehouses, taking into account population density and suitable locations. Identifying distribution points will also
 715 facilitate better organisation of aid efforts. Vulnerable groups, particularly children and those who have
 716 experienced psychological trauma, should be prioritised in these assistance initiatives.

717 The affected areas, especially the eastern part of District 1 where reinforced concrete structures is prevalent, may
 718 encounter challenges in road clearance, as traditional methods such as shovels and wheelbarrows may prove
 719 insufficient. Similarly, areas on the outskirts, characterised by a high volume of construction debris, will require
 720 more advanced road clearance equipment.

721

722 5. Conclusions

723 This study undertook a comprehensive multi-hazard analysis for Tabriz, employing a historical earthquake
 724 scenario and a GIS-based hazard model. By integrating demographic, structural, and seismic risk maps, the
 725 research identified the extent of structural damage, road blockages, and landslide-prone zones. For the first time,
 726 the study quantified the combined impact of landslides and structural collapse on road blockages, conducted a
 727 post-disaster accessibility analysis, and assessed the city's resilience to multi-hazard crises.

728 Our findings reveal that unauthorized constructions, non-compliance with urban planning principles, and
 729 development in fault zones significantly increase vulnerability, particularly for children and the elderly in
 730 economically disadvantaged areas. The study highlights the urgent need for targeted disaster preparedness, urban
 731 planning reforms, and improved resource allocation for emergency response.

732 The insights provided by this research are pivotal for city managers in formulating actionable strategies to reduce
 733 mortality and enhance rescue operations. Raising community awareness and resilience is particularly critical for
 734 vulnerable populations in the suburbs of Tabriz. However, the study faced limitations due to incomplete or

735 inaccurate data, a common challenge in developing countries. Addressing these data gaps is vital for more precise
736 risk assessments.

737 For future research, the impact of road loss on evacuation should be examined in greater depth, with a dedicated
738 study providing precise quantitative results. This is a crucial aspect of emergency response, requiring detailed
739 discussions and actionable recommendations to improve evacuation strategies during multi-hazard events.
740 Moreover, future studies should focus on integrating key infrastructure networks—such as water, sewage, and
741 power transmission—into the hazard model. The application of deep learning methods could further refine risk
742 predictions by reducing human error and increasing model accuracy, making the system more intelligent and
743 responsive to real-time disaster scenarios.

744

745 **Declaration of competing interest**

746 The authors declare that they have no known competing financial interests or personal relationships that could
747 have appeared to influence the work reported in this paper.

748

749 **Data availability**

750 The data used in this analysis is subject to confidentiality.

751

752 **Acknowledgment**

753 During the preparation of this work the author(s) used ChatGPT in order to improve language, readability and
754 proofreading. After using this tool/service, the author(s) reviewed and edited the content as needed and take(s)
755 full responsibility for the content of the publication.

756

757 **References**

- 758 [1] S. Karimzadeh, M. Ghasemi, M. Matsuoka, K. Yagi, A. C. Zulfikar, A Deep Learning Model for Road
759 Damage Detection After an Earthquake Based on Synthetic Aperture Radar (SAR) and Field Datasets,
760 IEEE Journal of Selected Topics in Applied Earth Observations and Remote Sensing. 15 (2022) 5753-
761 5765, Doi: 10.1109/JSTARS.2022.3189875.
- 762 [2] S. Cho, H. Xiu, M. Matsuoka, Backscattering Characteristics of SAR Images in Damaged Buildings Due
763 to the 2016 Kumamoto Earthquake. Remote Sens. 15 (2023) 2181, Doi.org/10.3390/rs15082181.
- 764 [3] D. Omarzadeh, S. Karimzadeh, M. Matsuoka, B. Feizizadeh, Earthquake Aftermath from Very High-
765 Resolution WorldView-2 Image and Semi-Automated Object-Based Image Analysis (Case Study:
766 Kermanshah, Sarpol-e Zahab, Iran). Remote Sensing. 13 (2021) 4272. Doi.org/10.3390/rs13214272.
- 767 [4] H. Vaidya, T. Chatterji, SDG 11 sustainable cities and communities.” Actioning the Global Goals for
768 Local Impact. Springer, Singapore. (2020) 173–185.
- 769 [5] M. Haghani, M.A. Shabani, M.S. Mesgari, Developing a Comprehensive Earthquake Preparedness
770 Framework for Schools in Iran: Lessons Learned from Past Earthquakes. Natural Hazards. 104 (2020)
771 1989-2010.

- 772 [6] Z. Wenchao, Q. Wang, X. Feng, Performance-Based Seismic Design and Assessment for Buildings in
 773 Urban Areas. *Seismic Design of Buildings to Eurocode*. 8 (2020) 253-267
- 774 [7] A. Tilloy, B. D. Malamud, H. Winter, A. Joly-Laugel, A review of quantification methodologies for
 775 multi-hazard interrelationships, *Earth-Science Reviews*, 196 (2019) 102881.
 776 <https://doi.org/10.1016/j.earscirev.2019.102881>.
- 777 [8] M. S. Kappes, M. Keiler, K. von Elverfeldt, T. Glade, Challenges of analyzing multi-hazard risk: A
 778 review, *Natural Hazards*, 64 (2012) 1925-1958. <https://doi.org/10.1007/s11069-012-0294-2>.
- 779 [9] L. Moya, E. Mas, F. Yamazaki, W. Liu, S. Koshimura, Statistical Analysis of Earthquake Debris Extent
 780 from Wood-Frame Buildings and Its Use in Road Networks in Japan. *Earthq.* 36 (2020) 209–231.
- 781 [10] W. Wang, N. Zhang, L. Wang, L. Z. Wang, D. Ma, A Study of Influence Distance and Road Safety
 782 Avoidance Distance from Postearthquake Building Debris Accumulation. *Adv. Civ. Eng.* (2020)
 783 7034517.
- 784 [11] J.W. Zhu, X.Z. Li, W.K. Xue, Y.C. Guo, Research on Emergency Response to Road Blockage Caused
 785 by Earthquake. *Advances in Engineering Research*. 540 (2020) 298-302.
- 786 [12] U. Takashi, The Great Hanshin-Awaji Earthquake and the Problems with Emergency Medical Care. *Ren.*
 787 *Fail.* 19 (1997) 633–645.
- 788 [13] M. Mavrouli S, Mavroulis, E. Lekkas, A. Tsakris, The Impact of Earthquakes on Public Health: A
 789 Narrative Review of Infectious Diseases in the Post-Disaster Period Aiming to Disaster Risk
 790 Reduction. *Microorganisms*. 11 (2023) 419. <https://doi.org/10.3390/microorganisms11020419>.
- 791 [14] F. Audemard, T. Azuma, F. Baiocco, S. Baize, A.M. Blumetti, E. Brustia, J. Clague, V. Comerci, E.
 792 Esposito, L. Guerrieri, L. Earthquake Environmental Effect for Seismic Hazard Assessment: The ESI
 793 Intensity Scale and the EEE Catalogue. *Mem. Carta Geol. D' Ital.* 97 (2015) 5–8.
- 794 [15] S. Karimzadeh, B. Feizizadeh, M. Matsuoka, From a GIS-based hybrid site condition map to an
 795 earthquake damage assessment in Iran: Methods and trends. *Int. J. Disaster Risk Reduct.* 22 (2017) 23–
 796 36.
- 797 [16] F. Audemard, T. Azuma, F. Baiocco, S. Baize, A.M. Blumetti, E. Brustia, J. Clague, V. Comerci, E.
 798 Esposito, L. Guerrieri, L. Earthquake Environmental Effect for Seismic Hazard Assessment: The ESI
 799 Intensity Scale and the EEE Catalogue. *Mem. Carta Geol. D' Ital.* 97 (2015) 5–8.
- 800 [17] Y. Tang, S. Huang, Assessing seismic vulnerability of urban road networks by a Bayesian network
 801 approach, *Transportation Research Part D: Transport and Environment*. 77 (2019) 390-402,
 802 <https://doi.org/10.1016/j.trd.2019.02.003>.
- 803 [18] Y. Zhou, J. Wang, J. Sheu, On connectivity of post-earthquake road networks, *Transportation Research*
 804 *Part E: Logistics and Transportation Review*. 123 (2019) 1-16, <https://doi.org/10.1016/j.tre.2019.01.009>.
- 805 [19] O. El-Anwar, J. Ye, W. Orabi, Efficient Optimization of Post-Disaster Reconstruction of Transportation
 806 Networks. *J. Comput. Civ. Eng.* 30 (2016) 0887–3801.
- 807 [20] D.A. McEntire, Impacts of Earthquakes on Critical Infrastructure. In *Earthquakes and Their Impact on*
 808 *Society*. (2019) 123-141.
- 809 [21] S. Sato, H. Ito, Y. Takahashi, Road Blockages Caused by Natural and Man-made Disasters and
 810 Countermeasures: A Review, *Journal of Disaster Research*. 16(2021), 908-919.
- 811 [22] T. Ikeda, D. Nohara, M. Tatsuta, T. Yamada, Towards Quantifying the Impacts of the 2018 Hokkaido
 812 Eastern Iwate Earthquake on Road Networks. *Natural Hazards and Earth System Sciences*, Volume 19
 813 (2019) 1961-1971.
- 814 [23] Y. Zhai, S. Chen, Q. OuYang, GIS-Based Seismic Hazard Prediction System for Urban Earthquake
 815 Disaster Prevention Planning. *Sustainability*, 11(2019) 2620.
- 816 [24] K. Liu, GIS-based MCDM framework combined with coupled multi-hazard assessment for site selection
 817 of post-earthquake emergency medical service facilities in Wenchuan, China, *International Journal of*
 818 *Disaster Risk Reduction*. 73 (2022) 102873, doi.org/10.1016/j.ijdr.2022.102873.
- 819 [25] C.Y. Lam, K. Tai, A.M. Cruz, Topological network and GIS approach to modeling earthquake risk of
 820 infrastructure systems: A case study in Japan, *Applied Geography*. 127 (2021) 102392,
 821 doi.org/10.1016/j.apgeog.2021.102392.
- 822 [26] M. Hashemi, A.A. Alesheikh, A GIS-based earthquake damage assessment and settlement methodology.
 823 *International Journal of Geographical Information Science*. 25 (2011) 1221-1235,
- 824 [27] Skilodimou, H.D., Bathrellos, G.D., Chousianitis, K. et al. multi-hazard assessment modeling via multi-
 825 criteria analysis and GIS: a case study. *Environ Earth Sci.* 78 (2019) 47, [https://doi.org/10.1007/s12665-](https://doi.org/10.1007/s12665-018-8003-4)
 826 [018-8003-4](https://doi.org/10.1007/s12665-018-8003-4)
- 827 [28] Rehman, A.; Song, J.; Haq, F.; Mahmood, S.; Ahamad, M.I.; Basharat, M.; Sajid, M.; Mehmood, M.S.
 828 Multi-Hazard Susceptibility Assessment Using the Analytical Hierarchy Process and Frequency Ratio
 829 Techniques in the Northwest Himalayas, Pakistan. *Remote Sens.* 14 (2022) 554,
 830 <https://doi.org/10.3390/rs14030554>

- 831 [29] S.N. Shorabeh, M.K. Firozjaei, O. Nematollahi, H.K. Firozjaei, M. Jelokhani-Niaraki, A risk-based
832 multi-criteria spatial decision analysis for solar power plant site selection in different climates: A case
833 study in Iran. *Renew. Energy*. 143 (2019) 958–973.
- 834 [30] D. Shahpari Sani, M.T. Heidari, H. Tahmasebi Mogaddam, S. Nadizadeh, S. Yousefvand, A. Karpour,
835 J. Jokar Arsanjani, An Assessment of Social Resilience against Natural Hazards through Multi-Criteria
836 Decision Making in Geographical Setting: A Case Study of Sarpol-e Zahab, Iran. *Sustainability*. 14
837 (2022) 8304.
- 838 [31] R. Afsari, S. Nadizadeh, M. Kouhnavard, M. Homaei, J.J. Arsanjani, A spatial decision support approach
839 for flood vulnerability analysis in urban areas: A case study of Tehran. *ISPRS Int. J. Geo-Inf.* 11 (2022)
840 380.
- 841 [32] I. Kougkoulos, S.J. Cook, V. Jomelli, L. Clarke, E. Symeonakis, J.M. Dortch, L.A. Edwards, M. Merad,
842 Use of multi-criteria decision analysis to identify potentially dangerous glacial lakes. *Sci. Total Environ.*
843 621 (2018) 1453–1466.
- 844 [33] Rahman, G.; Rahman, A.U.; Collins, A. Geospatial analysis of landslide susceptibility and zonation in
845 shahpur valley, eastern hindu kush using frequency ratio model. *Proc. Pak. Acad. Sci.* 54 (2017) 149–
846 163.
- 847 [34] George D. Bathrellos, Hariklia D. Skilodimou, Konstantinos Chousianitis, Ahmed M. Youssef,
848 Biswajeet Pradhan, Suitability estimation for urban development using multi-hazard assessment map,
849 *Science of The Total Environment*. 575 (2017) 119-134,
850 <https://doi.org/10.1016/j.scitotenv.2016.10.025>.
- 851 [35] Karpouza, M., Chousianitis, K., Bathrellos, G.D. et al. Hazard zonation mapping of earthquake-induced
852 secondary effects using spatial multi-criteria analysis. *Nat Hazards* 109 (2021) 637–669.
853 <https://doi.org/10.1007/s11069-021-04852-0>
- 854 [36] D.S. Fernández, M.A. Lutz, Urban flood hazard zoning in Tucumán Province, Argentina, using GIS and
855 multicriteria decision analysis. *Eng. Geol.* 111 (2010) 90–98.
- 856 [37] H. Karaman, integrated multi-hazard map creation by using AHP and GIS. 7th International Conference
857 on NATURAL HAZARDS (NAHA '15). 40 (2015) 101–110.
- 858 [38] A. Aghanabati, *The Geology of Iran; Geological Survey of Iran: Tehran, Iran.* (2004) 586.
- 859 [39] S. Karimzadeh, M. Miyajima, R. Hassanzadeh, R. Amir Aslanzadeh, B.A. Kamel, GIS-Based Seismic
860 Hazard, Building Vulnerability and Human Loss Assessment for The Earthquake Scenario in
861 Tabriz. *Soil Dyn. Earthq. Eng.* 66 (2014) 263–280.
- 862 [40] KDMC, karmani User Manual. Kerman Disaster Management Center. Kerman, Iran. 235 (2008).
- 863 [41] M. Ghasemi, S. Karimzadeh, M. Matsuoka, B. Feizizadeh, What Would Happen If the M 7.3 (1721) and
864 M 7.4 (1780) Historical Earthquakes of Tabriz City (NW Iran) Occurred Again in 2021? *ISPRS*
865 *International Journal of Geo-Information*. 10 (2021) 657, <https://doi.org/10.3390/ijgi10100657>.
- 866 [42] T.L. Saaty, *The Analytical Hierarchy Process, Planning, Priority: Resource Allocation.* Pittsburgh, PA:
867 RWS Publications. (1980).
- 868 [43] A. Mohajer Ashjai, A.A. Noroozi, 1978. Observed and probable intensity Zoning of Iran.
869 *Tectonophysics*. 49 (1978) 149–160.
- 870 [44] A.A. Nowroozi, Empirical relations between magnitudes and fault parameters for earthquakes in Iran.
871 *Bulletin of the Seismological Society of America*. 75 (1985) 1327–1338.
- 872 [45] V. Chandra, J.H. Whorter, A.A. Nowroozi, Attenuation of intensities in Iran. *Bull. Seismol. Soc. Am.* 69
873 (1979) 237–250.
- 874 [46] Japan International Cooperation Agency (JICA) & Centre for Earthquake and Environmental Studies of
875 Tehran (CEST) & Tehran Municipality. The study on seismic microzoning of the Greater Tehran area in
876 the Islamic Republic of Iran. Final report. (2000).
- 877 [47] R.N. Hassanzadeh, A. Zorica, R. Alavi Razavi, M. Norouzzadeh, H. Hodhodkian, Interactive Approach
878 for GIS-based Earthquakes Scenario Development and Resource Estimation (Karmania Hazard Model),
879 *Computers & Geosciences*. 51 (2013) 324–338.
- 880 [48] Z. Beheshti, A. Gharagozlou, M. Monavari, M. Landslides behavior spatial modeling by using evidential
881 belief function model, Promethean II model, and index of entropy in Tabriz, Iran. *Arab J Geosci.* 14
882 (2021) 1801, <https://doi.org/10.1007/s12517-021-08172-2>.
- 883 [49] C.N. Lin, A Fuzzy Analytic Hierarchy Process-Based Analysis of the Dynamic Sustainable Management
884 Index in Leisure Agriculture. *Sustainability*, 12 (2020) 5395.
- 885 [50] M. Hashemi, A. Asghar Alesheikh, A GIS-based earthquake damage assessment and settlement
886 methodology, *Soil Dynamics and Earthquake Engineering*. 31 (2011) 1607-1617,
887 doi.org/10.1016/j.soildyn.2011.07.003.
- 888 [51] M. Ghasemi, S. Karimzadeh, B. Feizizadeh, Urban classification using preserved information of high
889 dimensional textural features of Sentinel-1 images in Tabriz, Iran. *Earth Sci Inform.* 14 (2021) 1745–
890 1762, <https://doi.org/10.1007/s12145-021-00617-2>.

891 [52] A. Coburn, Spence, R. Earthquake Protection, 2nd ed.; John Wiley and Sons Ltd.: West Sussex, UK,
892 (2002).
893
894

Journal Pre-proof

Declaration of interests

The authors declare that they have no known competing financial interests or personal relationships that could have appeared to influence the work reported in this paper.

The authors declare the following financial interests/personal relationships which may be considered as potential competing interests:

Journal Pre-proof